Robust Optimization of a Post-combustion CO_2 Capture Absorber Column under Process Uncertainty

by

Ilse Mariana Cerrillo Briones

A thesis

presented to the University of Waterloo

in fulfillment of the

thesis requirement for the degree of

Master of Applied Science

in

Chemical Engineering

Waterloo, Ontario, Canada, 2019

AUTHOR'S DECLARATION

I hereby declare that I am the sole author of this thesis. This is a true copy of the thesis, including any required final revisions, as accepted by my examiners.

I understand that my thesis may be made electronically available to the public.

Abstract

In recent years, greenhouse gas (GHG) emissions is a global concern due to high concentrations of these gases in the atmosphere. Carbon capture and storage (CCS) has been suggested as an attractive alternative to curb intensive CO_2 emissions and reduce its impact to the environment. CCS technologies provide a direct alternative to reducing the emissions from coal and gas-fired power generation plants. However, in order to implement commercial-scale CO_2 capture plants, further studies are needed to mitigate all possible costs of this technology such as high energy consumption.

This work presents a study on a robust design optimization framework for a pilot-scale absorber column in post-combustion CO_2 capture. A mechanistic model describing the behaviour of a post-combustion CO_2 absorber column is explicitly considered. The proposed formulation takes into account uncertainty that will impact the absorber column due to seasonal or unexpected changes in the operating policies of a fossil-fired power plant, e.g., changes in the flue gas stream, as well as uncertainty associated with the physical thermodynamic properties of the species involved in the absorption process. Furthermore, in addition to the presence of model uncertainty, a multi-objective optimization in a multi-period scenario explicitly describing year-long seasonal changes in flue gas has been considered.

Different scenarios were assessed in order to evaluate the impact of uncertainty and multi-period changes on the optimal multi-objective process design. Optimal design specifications between different number of uncertain realizations and periodical changes were studied. However, higher computational demands were observed under extensive evaluations of uncertainty.

Results from this study suggest that larger dimensions in design are required when the optimization was evaluated under uncertainty and under multi-periods scenarios considering

uncertainty. The results show that the optimal design considering uncertainty and seasonal changes will be able to comply with the CO_2 capture policies. Thus, post-combustion CO_2 capture systems must be designed under these conditions to ensure feasibility of these plants during operation.

Acknowledgements

I would like to thank my supervisor, Prof. Luis Ricardez-Sandoval, for giving me the opportunity to pursue the MASc degree in University of Waterloo and his continuous guidance and support.

I would also like to extend my thanks the readers of my thesis, Professor Peter Douglas and Professor Jason Grove.

I'm especially grateful to my family in Mexico City for always showing unconditional love and support. I would also like to thank the Ricardez-PSE group for their constant support and friendship making this journey a very pleasant experience.

Finally, I appreciate for the financial support from the Mexican National Council for Science and Technology and Natural Sciences and Engineering Research Council (NSERC).

Dedicated to my beloved parents and sister.

Table of Contents

List of Figures

List of Tables

Nomenclature

List of English symbols

1NM	1-norm method
A	Guthrie's correlation parameters
$a_{g/l}$	Specific gas-liquid interfacial area
$a_{g/l}{}^*$	Specific gas-liquid interfacial area constraint
B	Guthrie's correlation parameters
CEPCI	Chemical Engineering Plant Cost Index
C_{tot}^{g}	Total molar concentration
Cp_i	Heat capacity
C_i^g	Molar concentrations of component *i* in the gas phase
C_i^l	Molar concentrations of component *i* in the liquid phase
C_{MEA}^*	Liquid molar concentration of free MEA
CO_2*	CO_2 capture target
C_{MEA}	MEA degradation cost
d	Design decision variables
D_{CO_2}	Diffusivity of CO_2 in the aqueous MEA solution
E_{abs}	Enhancement factor
$\overline{EL}$	Mean annual energy load in the province of Alberta
EL_p	Monthly energy load
f	Absorption column equality constraints
f_1	Maximization objective function
f_2	Minimization objective function

$\widehat{f_1}$	Normalized equation f_1
$\widehat{f_2}$	Normalized equation f_2
$f_{1\_CO_2}$	CO_2 capture maximization objective function
f_{2_CC}	Minimization cost objective function
$\widehat{f_{1\_CO_2}}$	Normalized CO_2 capture maximization function
$\widehat{f_{2\_CC}}$	Normalized Minimization cost function
Fg	Gas phase flowrate
Fg_p^0	Flue gas flowrate for multi-period scenario
Fg^0	Flue gas flowrate
$Fg_{CO_2}^0$	Molar flowrate of CO_2 in the flue gas
$Fg_{CO_2}^h$	Molar flowrate of CO_2 in the vent gas
Fl	Liquid phase flowrate
Fl_{MEA}	MEA inlet flowrate
h	Operational or environmental constrains
$h_{g/l}$	Interfacial heat transfer coefficient
He_i	Henry's constant of each species
He_{CO_2}	CO_2 Henry constant
h_{out}	Heat transfer coefficient from the absorber to the surroundings
i	Component (i.e., MEA, CO_2, H_2O, N_2)
J	Set of discrete realizations considered for the uncertain model parameters
k_2	Second-order overall reaction rate
$K_{g,i}$	Overall mass transfer coefficient in the gas phase
$k_{g,i}$	Binary mass transfer coefficients in the gas phase

$k_{l,i}$	Binary mass transfer coefficients in the liquid phase
k_{l,CO_2}	Liquid mass transfer coefficient of CO_2
LB	Lower bound
L/G	Liquid-to-gas ratio
L/G *	liquid-to-gas ratio constraint
MEA	Monoethanolamine
N_i	Mass transfer coefficient
P	Pressure of the column
p	Period in multi-period scenario
p_i	Partial pressure of each component
p_i^*	Equilibrium pressure in the gas-liquid phase
P_i^v	Species' vapour pressure
T_{amb}	Ambient temperature
T_g	Temperature of the gas phase
T_g^0	Flue gas temperature
u	Operating variables that can be adjusted during operation
UB	Upper bound
u_g	Mass velocity
u_l	Liquid velocity
w_j	Weight assigned for each realization in the uncertain parameters
X	Output space
x	State variables
$\dot{\mathbf{x}}$	Changes of the state variables with respect to the axial domain
x_i	Fraction in the liquid phase of species *i*

z	Axial domain

List of Greek symbols

ΔH_r	Heat of reaction per mol of CO_2
ΔH_{vap}	Heat of vaporization of H_2O
$\boldsymbol{\delta}$	Set of uncertain parameters
Θ_{min}	Minimization cost function
Θ_{max}	Maximization objective function
ε	epsilon constraint
Φ_{CC}	Cost function
γ_{CO_2}	Activity coefficient of CO_2
γ_{MEA}	Activity coefficient of MEA
γ_{H_2O}	Activity coefficient of H_2O
φ	Percentage of CO_2 capture
$\boldsymbol{\kappa}$	Model parameters

Chapter 1

Introduction

The increased concentration of major greenhouse gases (GHG) such as carbon dioxide (CO_2) are a direct consequence of anthropogenic activities. The ultimate objective of the U.N. Framework Convention on Climate Change (UNFCCC) is to stabilize GHG concentrations in the atmosphere at a level that would prevent dangerous anthropogenic interference with the climate system (Quadrelli and Peterson, 2007). The energy sector is largely dominated by the direct combustion of fuels, a process leading to large emissions of CO_2. Responsible of about 95% of the energy-related emissions, CO_2 from energy represents approximately 80% of the global anthropogenic GHG emissions (Quadrelli and Peterson, 2007).

Carbon capture and storage (CCS) provides a solution to these CO_2 intensive emissions, reducing the emissions from coal and gas-fired power generation plants. Current studies have focused on adjusting CCS technologies in order to make them economically feasible since nowadays these technologies consume significant amounts of energy. In order to improve CO_2 capture from gas or coal power generation, three main processes have been proposed: post-combustion capture, pre-combustion capture, and oxy-combustion. In post-combustion capture, CO_2 is separated from the power plant's flue gas produced from the combustion of fossil fuels. In pre-combustion capture, carbon is removed from the fuel before combustion, whereas in oxy-combustion, the fuel is burned in an environment of nearly pure O_2 (>95%) mixed with traces of nitrogen. Post-combustion capture offers some advantages as existing combustion technologies can still be used without major changes on their design and operating policies. Several techniques for post-combustion have been developed: chemical absorption, adsorption, membranes and cryogenic separation. Since the thermodynamic driving force for CO_2 capture from flue gas is low, chemical

absorption seems to be the most promising CCS alternative. Amines are able to capture CO_2 from streams with a low CO_2 partial pressure; this is because amines react with CO_2 to form water soluble compounds.

Amine-based CO_2 capture is one of the most studied technologies for CCS (Liang et al., 2015; Nwaoha et al., 2017; Tan et al., 2012; Wang et al., 2011). The amine based post-combustion basic process is shown in Figure 1. In this process, CO_2 is absorbed from a fuel gas or combustion gas near ambient temperature into an aqueous solution of amine with low volatility. The amine is regenerated in a stripping unit where the amine is separated from the CO_2 with water vapor at 100-120 °C; the amine is condensed from the stripper, leaving an almost pure CO_2 stream that can be compressed to 100 - 150 bar for geologic sequestration or CO_2 reutilization (Rochelle, 2009).

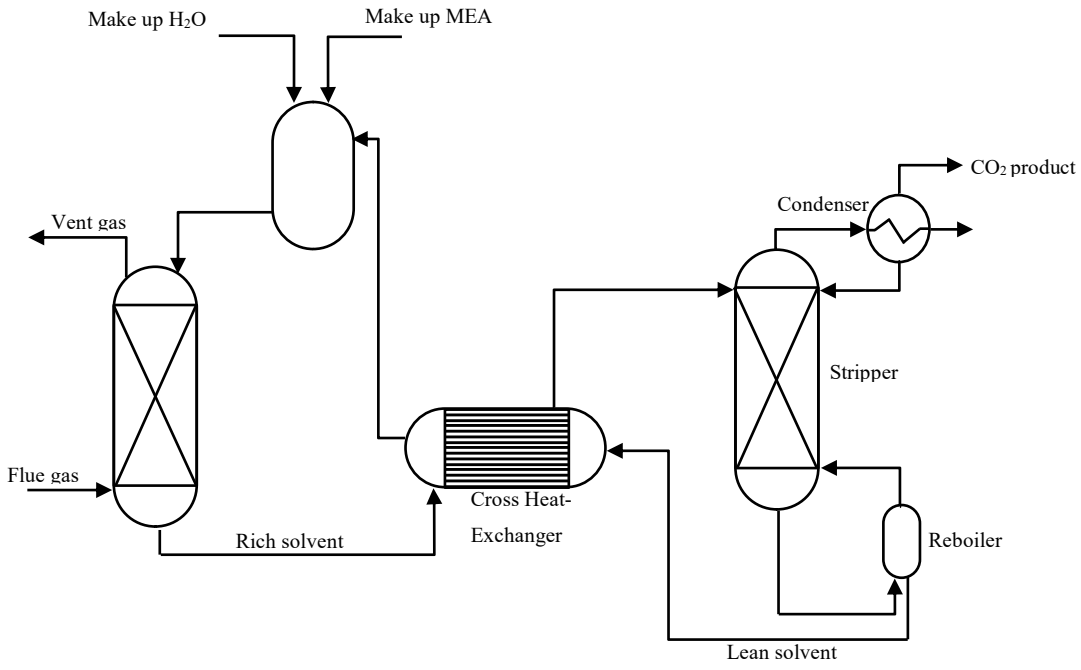

Figure 1 MEA post-combustion CO_2 capture process flowsheet

Since post-combustion CO_2 capture process was first introduced as a viable CCS technology, the energy penalty has been reduced by almost 50% (McCulloch et al., 2016). Hence, experimental research has been performed in order to evaluate process performance. While this approach will provide actual information about the system's behaviour, it may be costly and time consuming. In contrast, software and model simulation provides a low-cost and time-efficient alternative for post-combustion CO_2 research. Studies proposing mechanistic post-combustion CO_2 capture models have been previously reported in the literature (Harun et al., 2011; Kvamsdal et al., 2009; Mac Dowell and Shah, 2013; Nittaya et al., 2014; Prölß et al., 2011). Moreover, model development has advanced the study of optimal design and operations management policies for post-combustion systems. In most of those works, single-objective design optimization has been considered (Chu et al., 2016; Gaspar and Loldrup, 2016; Mores et al., 2012, 2018; Thouchprasitchai et al., 2018). Furthermore, efforts to establish a more flexible though efficient CO_2 capture process have been addressed through the formulation of multi-objective optimization problems (Bernier et al., 2010; Cristóbal et al., 2012; Eslick and Miller, 2011; Fazlollahi and Maréchal, 2013; Haghpanah et al., 2013; Harkin et al., 2012; Li et al., 2006) . Despite the efforts of optimizing the operating conditions for this process, the impact of uncertainty and external perturbations that may impact this process during operation can have a significant effect on process optimality and feasibility. Thus, optimization at nominal conditions, i.e. uncertain parameters set at their nominal values, may lead to suboptimal (or even inoperable) conditions when they are subject to parameter uncertainty and process disturbances. To this regard, the only study available is that of Bahakim and Ricardez-Sandoval, (2015) who developed a single-objective design optimization under uncertainty formulation for this process. Furthermore, previous design optimization studies have not considered of seasonal changes in the operation of the power plants.

Additionally, the implementation of the CO_2 capture process on conventional chemical engineering software programs such as Aspen HYSYS may be a straightforward alternative to simulate chemical systems; however, performing optimization of these systems while using that software may result in convergence problems, particularly when equipment sizing decisions are part of the degrees of freedom in the optimization formulation. Consequently, direct implementation of mechanistic process models in an optimization-oriented modelling language, e.g., PYOMO or GAMS, can improve model convergence if good initial conditions are provided.

1.1 Research Objectives

The objective of this study is to present a robust design optimization framework for an absorber column of a post-combustion CO_2 capture process. The novelty of this work is that it explicitly considers a mechanistic model describing the dynamic behaviour of a post-combustion CO_2 absorber column, uncertainty in both the process inputs and model parameters, and a multi-objective analysis. The robust multi-objective problem will be evaluated within a seasonal multi-period scenario performance of the CO_2 absorber in order to determine the optimal design conditions that will compensate for these changes. The expected contributions of addressing process uncertainty, multi-objective optimization and multi-period scenario to the design optimization framework is to guarantee that the proposed solutions will accommodate the possible scenarios that a real-life process can experience.

1.2 Structure of Thesis

This thesis is organized as follows: Chapter 2 provides a detailed literature review, outlining the previous works addressing post-combustion CO_2 capture process optimization, i.e. single objective optimization and multiobjective optimization. Moreover, a description of the multi-

objective method considered in this work, as well as previous contributions on multi-objective optimization of post combustion CO_2 capture are described in this section of the thesis.

Chapter 3 presents a robust design and operability optimization of a CO_2 capture mechanistic absorber model under uncertainty. A detailed mechanistic model describing the CO_2 absorber model is presented. Robust design optimization where uncertainty is considered in key input variables and model parameters is addressed to the CO_2 capture process. A study of the sensitivity of key process parameters to the optimal solution is also presented in this section of the thesis.

Chapter 4 presents a multi-objective optimization framework to a multi-period scenario of the CO_2 capture absorber column. The CO_2 capture absorber model described in section 3 is embedded within a multi-period scenario under uncertainty formulation where a robust multi-objective optimization formulation is considered. The aim of this study is to obtain the optimal design and operating conditions in order for the absorber column to recover the most CO_2 possible at low cost. This optimal design is evaluated with a specific technique to obtain the optimal solution between the two compromising objectives.

Chapter 5 summarizes the results of this thesis and presents the conclusions. Based on the scope considered for this present research, recommendations are provided for future work in the area of design optimization under uncertainty for CO_2 capture plants.

Chapter 2

Literature Review

Solvent-based post-combustion CO_2 capture is considered the most mature CO_2 technology; thus, control and optimization of this process has been extensively studied in the literature. Design optimization of this process has been recurrently studied, since it is crucial to determine the optimal design specifications and operating conditions that would make this technology economically viable and attractive. In this chapter, a review on the recent studies in design optimization for post-combustion CO_2 capture system is discussed. Also, a review on multi-objective optimization studies on the CO_2 capture process is presented. Furthermore, the multi-objective decision maker technique considered in this study is described in this section.

2.1 Post-combustion CO_2 capture

Post-combustion CO_2 capture modeling has been extensively studied in the literature; numerous approaches have been considered in order to determine the most effective way to describe the behaviour of this process.

In recent years, researchers have proposed dynamic models for MEA CO_2 capture processes, which makes dynamic models the latest emerging approach in this area. Lawal et al., (2009) presented a dynamic modelling study of the post combustion CO_2 capture absorber process. Two different approaches commonly studied for this process were compared to gain insight on the dynamic behavior of the absorber (i.e. the equilibrium-based approach and the rate-based approach). Results indicated that the rate-based model gives a better prediction of the chemical absorption process than the equilibrium-based model.

Gáspár and Cormoș, (2011) and Harun et al., (2012) presented detailed mechanistic models describing the complete process proposed as partial differential algebraic equations (PDAEs). Kvamsdal et al., (2009) proposed a similar detailed description for the packed column units, i.e. the absorber and stripper units. Details on how model parameters and physical properties were calculated were described in that work. The overall mass transfer coefficient including reactions of CO_2 is expressed only as a function of the enhancement factor. Those models were validated using steady-state pilot-plant data. To represent the actual operation of a power plant, the dynamic response of the MEA absorption processes were subjected to changes in the inlet flowrate similar to the actual process disturbances.

N. Mac Dowell, N.J. Samsatli, (2013) proposed a different approach to address a dynamic, non-equilibrium model of the absorption of CO_2 in an aqueous MEA solution. In order to account for all of the inter-species interactions in the fluid, including reactions, the SAFT-VR equation-of-state was considered. Steady state validation of the proposed model is performed using pilot plant data. The dynamic simulation was evaluated under the effect of changing the lean solvent flowrate and thermodynamic conditions of the lean solvent stream.

2.2 Design optimization of Post-combustion CO_2 capture units

Optimization of chemical and related processes requires a mathematical model that clearly describes and predict process behavior. In recent years, numerous studies have been published addressing the optimization of the post-combustion CO_2 capture process. In particular, the continuous interest for post-combustion CO_2 capture process using amine-based solvents has led to a number of research studies addressing the optimal design of these systems.

Mores et al., (2012) proposed a simultaneous optimization of operating conditions and the size

of the amine regeneration unit in the post- combustion CO_2 capture process. Three different concentrations of rich amine solution were considered by varying the CO_2 loading factor. The optimal solutions presented for three optimization problems clearly show that the functionalities of the most important process variables (operating conditions and dimensions) with CO_2 loading factor are smooth (linear, polynomial, exponential decay, exponential growth) and therefore can be accurately approximated using simple correlations, i.e. without the need of highly detailed models.

An industrial-scale CO_2 capture absorption column was investigated by Chu et al., (2016); in that work, the impact of the height, operating pressure and the packing materials of an absorbing column on the mass transfer performance and energy consumption was presented. The results show that the optimal operating pressure is the atmospheric pressure and the optimal height of the absorbing columns is about 8 m. For the minimum energy consumption, that study reported that the surface area per unit volume and the porosity of the packing materials should be as large as possible. Kang et al., (2016) performed a bi-objective optimization study for maximization of the net present value (NPV) and minimization of the total capital requirement (TCR) subject to a maximum CO_2 emission intensity constraint. Three solvent-based post-combustion CO_2 capture processes were evaluated, i.e. piperazine, mixed-salt and MEA. The results from that study indicate that, under equal capital cost scaling parameters, the piperazine and mixed-salt processes outperform the MEA process, and that the mixed-salt process in particular is quite promising. Mac Dowell and Shah, (2013) presented an optimization study aimed at identifying the cost-optimal degree of CO_2 capture using post-combustion amine-scrubbing integrated with a 660 MWe sub-critical coal fired power station. A non-equilibrium model of an absorption process was used in that study and implemented in gPROMS, which explicitly considered the trade-off associated with the cost of CO_2 emissions to the atmosphere against the opportunity

cost associated with reducing the electricity output of the power plant. That study reported that a 95% rate of CO_2 capture seems to be optimal.

Mores et al., (2018) proposed an optimization study of the decoupling between a natural gas combined cycle (NGCC) plant and a post-combustion CO_2 capture process by minimizing the mitigation cost defined as the ratio between the cost of electric power generation and the amount of CO_2 emitted per unit of total net electric power generated while satisfying design specifications, i.e. electric power generation capacity and CO_2 capture level. The results indicate that a fraction of the steam required in the reboiler of the amine regeneration process of the CO_2 capture plant has to be provided by steam turbines operating at an intermediate pressure level, whereas the other fraction needs to be provided by two evaporators of the heat recovery steam generators HRSGs.

In another study conducted by Rezazadeh et al., (2016), they proposed a rate-based model of the post combustion CO_2 capture process using an aqueous solution of 30 wt.% MEA as a representative pilot-scale capture plant. Those authors also performed a parametric sensitivity study. Several parameters were identified and varied over a given range of lean solvent CO_2 loading to evaluate their effects on the pilot plant energy requirement. The optimum lean solvent CO_2 loading was determined using the total equivalent work concept. Results show that, for a given packing material type, the majority of energy savings can be realized by optimizing the stripper operating pressure. To some extent, a higher solvent temperature at the stripper inlet has the potential to reduce the regeneration energy requirement. That study also showed that a more efficient packing material can greatly improve the pilot plant overall energy and mass transfer efficiency.

Mac Dowell and Shah, (2015) used a model of a super-critical coal-fired power plant integrated

with an amine-based CO_2 capture process to solve a multi-period dynamic optimization problem aimed at decoupling the operation of the power plant from the efficiency penalty imposed by the CO_2 capture plant. The objective was to maximize the decarbonized power plant's short run marginal cost profitability under four distinct scenarios: load following, solvent storage, exhaust gas by-pass and time-varying solvent regeneration. The study showed that, while the solvent storage option provides a marginal improvement of 4% in comparison to the load following scenario, the exhaust gas bypass scenario results in a profit reduction of 17%; nevertheless, the time-varying solvent regeneration option increases the profitability of the power plant by 16% in comparison to load following scenario.

Despite these efforts on identifying the optimal operating process parameters under constraints such as CO_2 capture policies, the effect of uncertainties on the optimal design for post-combustion CO_2 capture plants has not been extensively studied in the literature. Uncertainty may cause process designs, deemed to be optimal, to fail to achieve specific process design goals or even become inoperable in the presence of unexpected and sudden changes in the system.

To the author's knowledge, Bahakim and Ricardez-Sandoval, (2015) is the only study that has addressed the optimal design of large-scale CO_2 capture plant process under uncertainty. In that work, power series expansion (PSE) approximations were embedded within an optimization formulation to quantify process variability in a post-combustion CO_2 capture plant due to stochastic-based uncertainty. The plant model was implemented in Aspen HYSYS whereas the optimization framework was implemented in MATLAB. The results of that study showed that, to ensure a desired target CO_2 removal rate in the presence of process uncertainties, larger sizes for both the absorber and stripper towers as well as a higher reboiler heat duty are required. Based on the above, there is a motivation to study the optimal design of post-combustion CO_2 capture systems in the presence of uncertainty.

2.3 Optimization under uncertainty

The rapid development of computer science have enabled the solution of complex optimization problems in science and engineering (Sahinidis, 2004). In addition, events that cannot be explicitly predicted can be taken into account while performing optimization for various engineering applications. Stochastic programming is a popular method that considers uncertainty in the process by evaluating multiple realizations of the uncertain parameters by performing extensive simulations of the actual plant's model. In this approach, the uncertain parameters are often described using probability distribution functions (Birge and Louveaux, 1997). Different approaches addressing stochastic programming are available in the literature. In the multi-scenario method, the possible realizations of the uncertain model parameters are approximated into a set of discrete scenarios, each having a specific probability of occurrence or weight (Gomes et al., 2014). The constraints in the stochastic optimization problem are formulated such that they comply with the process specifications at a given probability limit (Bahakim and Ricardez-Sandoval, 2014; Rafiei and Ricardez-Sandoval, 2018; Ricardez-Sandoval, 2012). Another conventional stochastic optimization method widely used in engineering is two-stage optimization. In this approach, the decision variables of an optimization problem under uncertainty are partitioned into two sets. The first- stage decision variables are those that have to be decided before the actual realization of the uncertain parameters. Subsequently, once the uncertain parameters have been realized, further design or operational policy improvements can be made by selecting, at a certain cost, the values of the second-stage variables. Due to uncertainty, the second-stage cost is a random variable (Biegler et al., 1997; Ostrovsky et al., 2013). The objective is to choose the first-stage variables in a way that the addition of the first-stage costs and the expected value of the random second-stage costs are minimized (Sahinidis,

2004).

In general, the more uncertain realizations included in the optimization, the more accurate the results are expected to be at the expense of higher computational costs. However, accurate estimation of the expected objective function is computationally expensive as integration over a multi-dimensional space of uncertainty is required (Pintarič and Kravanja, 2004). Nevertheless, efforts have been made to alleviate such problems. For instance, different integration schemes have been presented in literature, e.g. the Gaussian quadrature formula and Monte Carlo simulation (Acevedo and Pistikopoulos, 1998). Similarly, Ostrovsky et al., (2011) developed an approximate method for solving the two-stage optimization problems where the constraints must be satisfied with some probability, i.e. chance constraints optimization (Arellano-Garcia and Wozny, 2009; Li et al., 2008).

While stochastic programming aims to identify solutions that will comply with the process constraints at a certain (user-defined) probability limit, there are some engineering applications that are required to be immune against model uncertainty, i.e., they are required to remain feasible for all the possible uncertain realizations at minimum cost. Another approach for the scenario-based optimization is robust optimization. In this approach, the process constraints are expected to be fully satisfied for every realization (i.e. scenario) considered in the uncertain parameters. Hence, robust optimization does not require information about the probability distribution of the uncertainty data. Nevertheless, the problem size will increase exponentially with the number of uncertain parameters, which restricts its application in solving problems with multiple uncertain parameters. Robust optimization promises to ensure robustness by enforcing the feasibility of an optimization problem for the entire given uncertainty space (Li and Ierapetritou, 2008; Lin et al., 2004). However, larger and more expensive designs and operating specifications are required in order to comply with all process constraints in the presence of

uncertainty. While robust optimization aims to ensure feasibility under process uncertainty, it may sometimes be more economical to comply all the time with key process constraints and allow violation of less critical constraints under uncertainty. In order to account for this penalty in process constraints, a ranking-based design approach that ensures feasibility of the critical higher ranked constraints at all times but allows less penalized constraints was proposed in the literature (Bahakim et al., 2014). In that method, the objective function aims to minimize the expected value and variance of the cost function whereas the constraints are redefined as minimum probability of satisfaction (or shape) in the presence of uncertainty (Bahakim et al., 2014). To the author's knowledge, studies involving the optimization under uncertainty for the optimal design of post-combustion plants are limited. As was mentioned in Section 2.2, Bahakim and Ricardez-Sandoval, (2015) is the only study that has addressed optimal design of large-scale CO_2 capture plant process under stochastic-based uncertainty. Thus, there is a lack of studies addressing the optimal design of post-combustion CO_2 capture systems under uncertainty. In the current study, a robust optimization approach is considered to ensure that process constraints remain feasible under uncertainty.

2.4 Multi-objective optimization

Optimization of chemical processes is essential for reducing material and energy requirements as well as the harmful environmental impact. It leads to better design and operation of chemical processes as well as to sustainable processes. However, many applications involving optimization can consider multiple objectives, some of which are conflicting with each other. Multi-objective optimization is required to solve the resulting problems in these applications (Rangaiah, 2009). Post-combustion CO_2 process has been extensively studied using single

objective optimization formulations; however, efforts in addressing multi-objective optimization in this process have also been addressed in the literature.

2.4.1 Multi-objective optimization: CO_2 capture processes

The relevance of multi-objective optimization in chemical engineering, particularly in CO_2 capture systems, is continuously growing. This has been partially motivated by the availability of new and effective methods for solving multi-objective problems as well as increased computational resources.

Bernier et al., (2010) presented a multi-objective optimization by iterative simulation in an integration of a CO_2 capture process using monoethanolamine (MEA) in a natural gas-combined cycle power plant, simultaneously optimizing column dimensions, heat exchangers, and absorbent flow configuration. Two optimization objectives were considered: the levelized cost of electricity and its life cycle global-warming potential. After optimization, the results showed that increasing the diameter of the absorber and generating near-atmospheric pressure steam are cost-effective options; in particular, complex stripper configurations such as split-flow and multi-pressure are less attractive when very low pressure steam is recovered by heat exchange and expanded in the condensing turbine. In another study, Eslick and Miller, (2011) examined the multi-objective optimization of a combined system of a coal power plant coupled with models of an MEA-based carbon capture system and a CO_2 compression system. The design optimization seeks to minimize freshwater consumption and levelized cost of electricity, so the trade-off between decreased water consumption and cost of electricity can be obtained under different design and operating parameters. The optimization of the combined system showed a wide range of potential Pareto-optimal designs meeting the design specifications of 90% capture.

Harkin et al., (2012) presented a model of an existing power station with a potassium carbonate-based carbon capture plant including CO_2 compression. The aim of that study was to optimise the net power output of the power station and amount of CO_2 captured for a range of solvent flowrates, lean loading and stripper pressures. After a Pareto analysis of the multi-objective optimization of the process it was identified that lean solvent loading and stripper pressure will have a large impact on the net power output and amount of CO_2 captured.

Lee et al., (2013), presented a multi-objective analysis for three amine solvents: monoethanolamine (MEA), diethanolamine (DEA), and 2-amino-2- methyl-1-propanol (AMP) in a 90% CO_2 capture process from a 550 MW coal fired power plant. The aim of that work was to determine sets of conditions that were best suited for each solvent to meet design objectives that maximize net power output of the power plant and minimize the capital cost investment of the CO_2 capture process. An analysis of the Pareto front for each amine trade-offs between the two conflicting objectives showed that best process specifications are solvent-dependent.

Li Yuen Fong et al., (2016), performed a multi-objective optimization technique, i.e., pareto analysis, in combination with heat integration to optimise the total shaft work and the overall CO_2 recovery rate in a hybrid capture system that combined both the capture and the compression units. The multi-objective optimisation provided a range of optimal solutions where the total shaft work increased with the total CO_2 being recovered by the hybrid process. However, a minimum optimum was determined for the total specific shaft work required at an overall recovery rate of 88.9%, which required 1.40 GJ/(t CO_2 captured).

Despite these efforts of implementing multi-objective optimal solutions to this process, there is still a limited focus on the decision maker techniques on choosing the optimal solution between the trade-off results in the presence of uncertainty.

2.4.2 Multi-objective Optimization: Solution strategies

There are two main types of methods to dealing with multi-objective optimization problems, a priori and a posteriori methods. A posteriori methods aim to provide a decision maker (DM) with efficient trade-off solutions called Pareto solutions. The decision maker can then afterwards look at the set of Pareto solutions provided and select one that complies with the process needs. In contrast to a posteriori methods, the decision maker's preferences are selected in advance in a priori methods; hence, a single trade-off solution is obtained after a unique search, rather than a having access to a set of solutions. Different multi-objective methods are then classified between these categories; comprehensive reviews on multi-objective methods can be found elsewhere (Collette and Siarry, 2003; Marler and Arora, 2007; Rangaiah, 2009). Thus, in order to determine an optimal solution in the present work, it is considered that a priori methods will be more suitable as they are considered practical methods for this matter.

In general, a multi-objective problem will have two or more objectives involving many decision variables and constraints. Consider a multi-objective problem with two objectives: $f_1(\mathbf{x})$ and $f_2(\mathbf{x})$, and several decision variables ($\mathbf{d}$). This problem, also referred to as bi-objective optimization problem, can be formulated as follows (Rangaiah, 2009):

$$
\begin{aligned}
&\underset{\mathbf{d}}{\text{Maximize}} && f_1(\mathbf{x}) \\
&\underset{\mathbf{d}}{\text{Minimize}} && f_2(\mathbf{x}) \\
&\text{s.t.} && h(\mathbf{x}) = 0 \\
& && g(\mathbf{x}) \le 0 \\
& && \mathbf{x} \in \mathbf{X} \\
& && \mathbf{d}^{L} \le \mathbf{d} \le \mathbf{d}^{U}
\end{aligned}
\qquad (1)
$$

Bi-objective optimization problems generate an infinite set of noninferior solutions which will define a trade-off curve (Figure 2). Thus, it is not possible to obtain a solution that simultaneously improves in the two objectives (Grossmann et al., 1982).

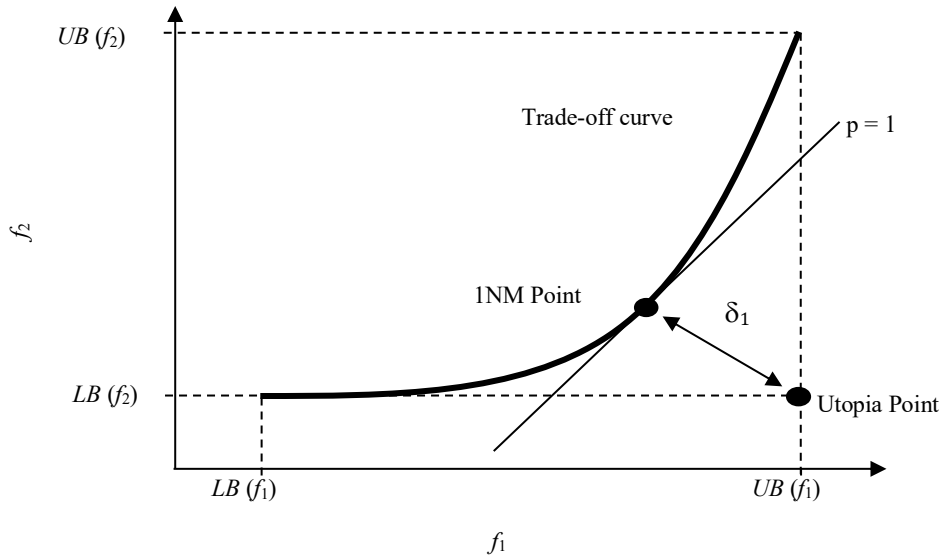

Figure 2. 1-norm minimum trade-off solution on trade-off surface

Assume problem (1) has a series of noninferior solutions, i.e., solutions where it is not possible to obtain a simultaneous improvement in the two objectives; in order to determine the optimal solution, two solution strategies can be considered. In the first method, a set of noninferior solutions are generated, next a decision maker will select an optimal solution. In the second strategy, a single solution compromising the two conflicting objectives is determined.

The first method, referred to as the ε-constraint method, is a common technique for generating noninferior solutions in which one of the objectives is optimized whereas the other objective is constrained to a threshold criterion ε, i.e.

$$
\begin{aligned}
&\underset{\mathbf{d}}{\text{Minimize}} && f_2(\mathbf{x}) \\
&\text{s.t.} && f_1(\mathbf{x}) \geq \varepsilon \\
& && h(\mathbf{x}) = 0 \\
& && \mathbf{x} \in \mathbf{X} \\
& && \mathbf{d}^L \leq \mathbf{d} \leq \mathbf{d}^U
\end{aligned} \qquad (2)
$$

By selecting different values of ε and solving problem (2), a set of noninferior configurations can be generated. This procedure will aid the decision maker in selecting an optimal trade-off solution.

The second method is an alternative strategy for solving bi-objective optimization problems by searching for an ideal compromised solution, in which both objectives sacrifice the least that is possible with respect to their maximum attainable benefit. This method is referred to as p norm method. (Grossmann et al., 1982).

In this approach, a reference point named utopia point will represent the output space of coordinates (UB (f 1), LB (f2)) as illustrated in Figure 2. Assume that UB (f_1) and LB (f_2) are the values of f_1 and f_2 when optimized respectively over the constraint set **X**. This utopia point since it lies outside the feasible output space **X**. The ideal solution will be determined by the noninferior solution which is closest to the utopia point. This requires that the distance between the utopia point and the noninferior solution be at a minimum. This distance δ_p, is determined by the p-norm from the utopia point. Since $1 < p < \infty$, it is often considered the two extreme norms when minimizing the distance between the noninferior solution and the utopia point (i.e., p=1 and p=∞). Therefore,

$$
\begin{aligned}
&\text{p=1:} && \min_{\mathbf{d}} \; (1 - \widehat{f_1}(\mathbf{x})) + \widehat{f_2}(\mathbf{x}) \\
&\text{s.t.} && h(\mathbf{x}) = 0 \\
& && g(\mathbf{x}) \leq 0
\end{aligned}
$$

$$\mathbf{x} \in \mathbf{X}$$
$$\mathbf{d}^{L} \le \mathbf{d} \le \mathbf{d}^{U} \quad (3)$$

p=∞: $\min_{\mathbf{d}} \max \left\{ \left(1 - \widehat{f_1}(\mathbf{x})\right), \widehat{f_2}(\mathbf{x}) \right\}$

s.t. $h(\mathbf{x}) = 0$

$g(\mathbf{x}) \le 0$

$\mathbf{x} \in \mathbf{X}$

$\mathbf{x}^{L} \le \mathbf{x} \le \mathbf{x}^{U} \quad (4)$

where $\widehat{f_1}(\mathbf{x})$ and $\widehat{f_2}(\mathbf{x})$ are normalizations of $f_1(\mathbf{x})$ and $f_2(\mathbf{x})$:

$$\widehat{f_1}(\mathbf{x}) = \frac{f_1(\mathbf{x}) - LB(f_1)}{UB(f_1) - LB(f_1)} \qquad \widehat{f_2}(\mathbf{x}) = \frac{f_2(\mathbf{x}) - LB(f_2)}{UB(f_2) - LB(f_2)} \quad (5)$$

While norm p=1 will always correspond to a noninferior point even if the output space is nonconvex, the solution may not necessarily be a noninferior point for the nonconvex case when p=∞. Therefore, in this work we will consider norm p=1 method (1NM) since it is an efficient and practical approach to obtain a compromise solution.

2.5 Summary

The optimization of solvent based post-combustion CO_2 capture has received attention in the last decades since it is critical to seek for the optimal design specifications and operating conditions under which this process will be attractive to the energy sector. The most commonly used approach for process design optimization is by optimizing a steady state model under one single objective and under the assumption of nominal conditions. However, this approach might result in sub-optimal conditions that can fail in the presence of process disturbances or uncertainty.

Efforts to consider uncertainty in design optimization studies have formally considered the formulation and optimization of design problems in order to obtain robust designs where all process constraints and uncertain parameters will remain feasible. However, in order to ensure a robust though optimal process design, high computational costs are expected and the efforts to reduce these costs is still an active area of research.

Current studies in post-combustion CO_2 capture focus in the optimization of this process; however, there is a lack of research on the impact that process disturbances and process uncertainty may have on the optimal process design of post-combustion CO_2 capture units. Likewise, as in any other process, the presence of different conflicting optimal targets is also an important factor to consider. Hence, multi-objective optimization formulations have been studied previously for the post-combustion CO_2 capture process. Despite these efforts, no specific optimal solutions are given to obtain a single trade-off solution under the conflicting objectives. Moreover, there is a lack of studies addressing uncertainty for a multi-objective design optimization of a post-combustion CO_2 capture process.

There are several methods that can be used by the decision maker to obtain an optimal solution under a set of Pareto optimal points for multi-objective optimization. However, the present study will consider the two methods described in the previous section (ε-constraint and 1NM method). These methods provide adequate optimal solutions to the problem of interest. This thesis will take into account process disturbances, process model uncertainty and multi-objective optimization for a multi-period post-combustion CO_2 absorber mechanistic model.

Chapter 3

Robust Design Optimization of a Post-combustion CO_2 Capture Absorber Column under Process Uncertainty

A conventional approach to address process uncertainty consist of accounting for overdesign factors; however, this method has shown to be sub-optimal (Koller et al., 2018; Rafiei and Ricardez-Sandoval, 2018). Recent studies have accounted for design, control and optimization under uncertainty through different strategies in other processes different to CO_2 capture process (Cignitti et al., 2018; GarciÌa-Herreros et al., 2011; Giannakoudis et al., 2010; Gomes et al., 2014; Li and Floudas, 2016; Mansouri et al., 2016; Patil et al., 2015; Ricardez-Sandoval et al., 2009; Yuan et al., 2016).

This section presents a robust design optimization framework for a pilot-scale absorber column in post-combustion CO_2 capture. A mechanistic model describing the behaviour of a post-combustion CO_2 absorber column is explicitly considered in the present robust design optimization formulation. Moreover, this work accounts for uncertainty that will impact the absorber column due to seasonal or unexpected changes in the operating policies of a fossil-fired power plant, e.g. changes in the flue gas stream, as well as uncertainty associated with the physical thermodynamic properties of the species involved in the absorption process. First a detailed description of the pilot-scale mechanistic CO_2 capture absorber model employed in this study is presented. This is followed by the robust design optimization formulation proposed in this work. Next, the model validation and the robust designs obtained under different scenarios are presented. A summary of the major outcomes obtained from this study is provided at the end.

3.1 Pilot-scale CO_2 capture absorber model

The process studied consist of a packed bed absorber column operating at atmospheric pressure, where the flue gas stream coming from a fossil power plant passes through it. The flue gas is contacted directly with the lean amine solution (30% w/w MEA) in the unit. A gas with reduced CO_2 content leaves the top of the absorber while the rich amine solution loaded with CO_2 leaves the unit from the bottom of the tower (Figure 3).

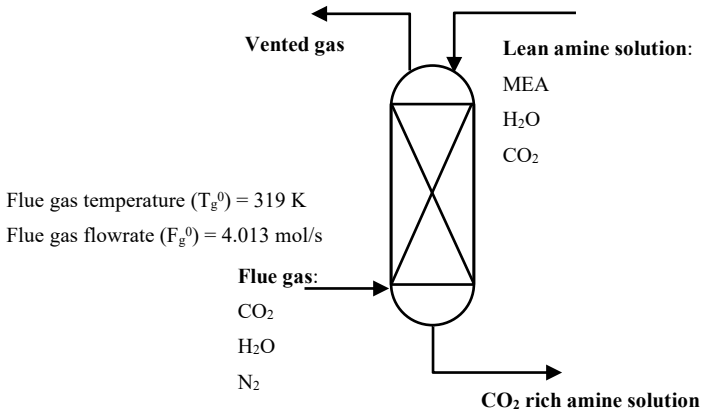

Figure 3 Process flow diagram of an MEA absorption process

The mathematical model describing this process was adapted from the model presented by Harun et al., (2012). The current model consists of a set of differential equations describing the spatial changes in the mass balance in the liquid and gas phase of each component involved in the process (i.e., MEA, CO_2, H_2O, N_2), as well as the energy balance of liquid and gas phases. The assumptions considered for this model are as follows:

1. The fluid within the column is turbulent flow and is approximated as a plug flow.
2. One-dimensional (axial domain) differential mass and energy balances for both gas and liquid phases.
3. Linear pressure drop (fixed outlet pressure).

4. Ideal gas phase due to low pressure.
5. No accumulation in gas and liquid films.
6. Fluxes of CO_2, H_2O and MEA between the gas and liquid phase are allowed in both ways.
7. Thermal equilibrium is assumed between the liquid and the gas phase.

3.1.1 Mass and heat balance

The mass component balances for the gas and liquid phases are as follows:

$$-C_i^g \frac{du_g}{dz} - u_g \frac{dC_i^g}{dz} - a_{g/l} N_i = 0 \quad (6)$$

$$-u_l \frac{dC_i^l}{dz} + a_{g/l} N_i = 0 \quad (7)$$

where C_i^g (mol/m^3) and C_i^l (mol/m^3) are the molar concentrations of component *i* in the gas and liquid phase, respectively; u_g (m/s) and u_l (m/s) are the gas and liquid velocities, respectively; $a_{g/l}$ (m^2/m^3) is the specific gas-liquid interfacial area. To account for the interfacial mass transport in the column, the molar flux, N_i (mol/m^2/s), defined as the net loss of component *i* in the gas phase and the gain of the same component in the liquid phase, is included in the model. The components *i* considered in the present absorber column model are monoethanolamine (MEA), nitrogen (N_2), carbon dioxide (CO_2) and water (H_2O); and *z* is the space domain. Note that nitrogen is not involved in the reaction and was not considered to be transferred between the two phases.

The total mass balance considers that the velocity of the gas phase changes across the axial domain of the column. This balance is as follows:

$$\frac{du_g}{dz} = -\frac{u_g}{P}\frac{dP}{dz} + \frac{u_g}{T_g}\frac{dT_g}{dz} - \frac{a_{g/l}}{C_{tot}^g}\sum N_i \quad (8)$$

where P (bar) is the pressure in the column, T_g (K) is the temperature of the gas phase and C_{tot}^g (mol/m^3) is the total molar concentration defined as follows:

$$C_{tot}^g = C_{CO_2}^g + C_{MEA}^g + C_{H_2O}^g + C_{N_2}^g \quad (9)$$

The energy balance equations for the gas and liquid phases are as follows:

$$-u_g \frac{\partial T_g}{\partial z} + \frac{a_{g/l}}{\sum(C_i^g Cp_i)} h_{g/l}\left(T_l - T_g\right) = 0 \quad (10)$$

$$-u_l \frac{\partial T_l}{\partial z} - \frac{a_{g/l}}{\sum(C_i^l Cp_i)}\left(h_{g/l}\left(T_l - T_g\right) - \Delta H_r N_{CO_2} - \Delta H_{vap} N_{H_2O} - h_{out}(T_l - T_{amb})\right) = 0 \quad (11)$$

where Cp_i (J/mol/K) is the heat capacity and $h_{g/l}$ (W/m^2/K) is the interfacial heat transfer coefficient. The heat transfer film coefficient ($h_{g/l}$) is estimated using the Chilton-Colburn analogy between heat and mass transfer (C. J. Geankoplis, 1993). ΔH_r (J/mol) is the heat of reaction per mol of CO_2, ΔH_{vap} (J/mol) is the heat of vaporization of H_2O and h_{out} (W/m^2/K) is the heat transfer coefficient for heat transferred from the absorber to the surroundings. The heat of reaction (ΔH_r) and the heat from the absorber to the surroundings (h_{out}) values were obtained from Kvamsdal and Rochelle, (2008); T_{amb} (K) is the ambient temperature.

3.1.2 Rate of mass transfer

The species' mass transfer coefficients at the gas-liquid interface is estimated using the following film model equations:

$$N_i = K_{g,i}(p_i - p_i^*) \qquad i=\{\text{MEA, } N_2, CO_2, H_2O\} \qquad (12)$$

$$\frac{1}{K_{g,i}} = \frac{1}{k_{g,i}} + \frac{He_i}{k_{l,i}E_{abs}} \qquad (13)$$

where $K_{g,i}$ is the overall mass transfer coefficient in the gas phase whereas $k_{g,i}$ and $k_{l,i}$ are the binary mass transfer coefficients in the gas and the liquid phases, respectively; p_i represents the partial pressure of each component and is a function of the total pressure in the column (P); similarly, p_i^* represents the equilibrium pressure in the gas-liquid phase; E_{abs} is the enhancement factor and He_i is the Henry's constant of each species. The use of an overall mass transfer coefficient for each species (N_i) eliminates the need to calculate the concentrations at the interface. The direction from the gas to the liquid phase was taken as the positive direction for mass transfer. The present model assumes that the resistance to mass transfer for both H_2O and MEA in the liquid phases is negligible, i.e. for components that have higher solubility such as H_2O and MEA, the major resistance for mass transfer occurs in the gas phase.

The chemical reactions that occurs in the MEA absorption process increases the rate of CO_2 absorption in the liquid phase. The present model considers chemical equilibrium in the bulk of the liquid phase to provide liquid phase compositions. The following reactions describing the species distribution are established (Austgen et al., 1989):

Carbamate reversion to bicarbonate:

$$MEACOO^+ + H_2O \longleftrightarrow MEA + HCO_3^-$$

MEA deprotonation:

$$MEAH^+ + H_2O \longleftrightarrow MEA + H_3O^+$$

Bicarbonate formulation:

$$CO_2 + 2H_2O \longleftrightarrow HCO_3^- + H_3O^+$$

Carbonate formulation:

$$HCO_3^- + H_2O \longleftrightarrow CO_3^{-2} + H_3O^+$$

Dissociation of water:

$$2H_2O \longleftrightarrow OH^- + H_3O^+ \qquad (14)$$

The overall effect of these reactions is considered in the liquid phase mass transfer through an enhancement factor (E_{abs}). This factor represents an approximated analytical solution of the differential equations governing the simultaneous diffusion mass transfer and chemical reactions in the liquid film. The enhancement factor is valid only in the pseudo first-order reaction regime with respect to the concentration of CO_2 (Kvamsdal et al., 2009). This condition is typically valid in a packed column absorbing CO_2 in an alkanolamine solution, due to the effective liquid mixing provided by the packing material. The pseudo first-order regime is facilitated by the combination of low CO_2 partial pressure, high reactant concentration and short contact time between each liquid mixing point. The volume of amine is considered to be constant throughout the liquid film and equal to the liquid volume in the bulk phase. Therefore, the enhancement factor (E_{abs}) for the absorber is estimated as follows:

$$E_{abs} = \frac{\sqrt{k_2 C_{MEA}^* D_{CO_2}}}{k_{l,CO_2}} \qquad (15)$$

where k_2 is the second-order overall reaction rate, C_{MEA}^* is the liquid molar concentration of free MEA, calculated from the equilibrium model proposed by Hoff et al., (2004), D_{CO_2} is the diffusivity of CO_2 in the aqueous MEA solution (te Riele et al., 1995), and k_{l,CO_2} is the liquid mass transfer coefficient of CO_2 (Onda et al., 1968).

The equilibrium model considered in this study is based on the coupling between phase equilibrium and chemical equilibrium. Phase equilibrium, which exists at the gas-liquid interphase, dominates the distribution of the molecular species between the vapour and liquid phases whereas chemical equilibrium describes the distribution of the molecular and ionic species in the liquid phase. For the H_2O and MEA, the equilibrium pressure in the gas-liquid interface is calculated as follows:

$$p_i^* = x_i \gamma_i P_i^v \quad (16)$$

where x_i is the fraction in the liquid phase of species *i* and P_i^v is the species' vapour pressure. In the case of CO_2, the temperature of the system exceeds its supercritical temperature, i.e., CO_2 does not exist as a liquid at that temperature. Therefore, Eq. (16) cannot be applied to model the partial pressure of CO_2. Instead, the equilibrium partial pressure of the CO_2, which is related to the free CO_2 concentration on the solution through Henry's law, is calculated as follows:

$$p_{CO_2}^* = He_{CO_2} C_{CO_2}^* \gamma_{CO_2} \quad (17)$$

where He_{CO_2} is the CO_2 Henry constant and γ_{CO_2} is the activity coefficient of CO_2.

3.1.3 Physical properties

The Henry constant (He_{CO_2}) of CO_2 in MEA solution was calculated using the N_2O correlation (Haimour and Sandall, 1984). The species' gas and the liquid mass transfer coefficients ($k_{g,i}$ and $k_{l,i}$) and gas-liquid interfacial area ($a_{g/l}$) were estimated using the correlation reported in Onda et

al., (1968) and it is not shown here for brevity. In this study, the empirical correlation proposed by Hikita et al., (1977) was used to estimate the second order overall reaction rate (k_2).

3.2 Optimal process design under uncertainty

The robust optimization framework considered in this work aims to search for the optimal design of the CO_2 capture absorber column in the presence of uncertainty. This formulation is as follows:

$$\min_{\mathbf{d},\mathbf{u}} = \sum_{j=1}^{J} w_j \left(\Phi_{CC}\left(\mathbf{d}, \boldsymbol{\kappa}_j, \mathbf{x}_j, \dot{\mathbf{x}}_j, \mathbf{u}, \boldsymbol{\delta}_j\right) \right)$$

s.t.

$$f\,(\mathbf{d}, \boldsymbol{\kappa}_j, \dot{\mathbf{x}}_j, \mathbf{x}_j, \mathbf{u}, \boldsymbol{\delta}_j) = 0 \qquad \forall j = 1, 2, \ldots J$$

$$h\,(\mathbf{d}, \boldsymbol{\kappa}_j, \dot{\mathbf{x}}_j, \mathbf{x}_j, \mathbf{u}, \boldsymbol{\delta}_j) \leq 0 \qquad \forall j = 1, 2, \ldots J$$

$$\mathbf{d}^l \leq \mathbf{d} \leq \mathbf{d}^u$$

$$\mathbf{u}^l \leq \mathbf{u} \leq \mathbf{u}^u \qquad (18)$$

where the objective function presented in (18) is described in terms of the capital and operating costs for the absorption column; **f** represents the absorption column equality constraints, i.e. the absorption column model presented in the previous section, whereas **h** represents the operational or environmental constrains considered in the formulation. Similarly, **d** are the process design variables, **κ** are the model parameters, **x** represents the state variables whereas $\dot{\mathbf{x}}$ represent the changes of the state variables with respect to the axial domain (z). The operating variables that can be adjusted during operation are denoted by **u** whereas **δ** represents the set of uncertain parameters. w_j represents a weight assigned for each realization in the uncertain

parameters, i.e., $\sum_{j=1}^{J} w_j = 1$. These weights can be estimated using a probabilistic distribution function for the uncertain parameters.

As shown in problem (18), a multi-scenario approach has been implemented in this work to address the optimal design and operation of the absorber column under uncertainty. This approach was selected because it is the most-widely used technique employed in the academia and the industry to account for uncertainty (Gomes et al., 2014; Karuppiah and Grossmann, 2006; Laird and Biegler, 2008; Wiecek et al., 2009; Zhu et al., 2010). The term J represents the set of discrete realizations or scenarios considered for the uncertain model parameters; accordingly, the cost function (Φ_{CC}), the process model equations and constraints (i.e. **f** and **g**) need to account for each realization (j) considered for the uncertain parameter set $\boldsymbol{\delta}$. In the present work, the height and diameter of the absorber column (i.e. H_{abs} and D_{abs}) are the main process design parameters **d** whereas the inlet flowrate (Fl_{MEA}) is most important operating condition that can be adjusted during operation. Therefore, these are the main variables used for optimization in the present formulation. The economic cost function considered for the absorber model is has been formulated based on Guthrie's (Guthrie, 1969) correlation and is as follows:

$$\Phi_{CC} = A * ROR \left(\frac{CEPCI}{B}\right) D_{abs}{}^{1.066} H_{abs}{}^{0.82} + Fl_{MEA} C_{MEA} \qquad (19)$$

where C_{MEA} denotes the MEA degradation cost due to the MEA loses in the post combustion process (5.38E-5 $/mol_MEA) (Huertas et al., 2015; Singh et al., 2003). A and B represent the Guthrie's correlation parameters, i.e. 290.82 and 280, respectively. The present economic function is annualized using a 20% rate of return (ROR = 0.2). CEPCI represents the Chemical Engineering Plant Cost Index (723.5 for May of 2018) (Engineering and Cost, 2018).

A CO_2 capture process is known to be efficient based on its ability to capture CO_2 for the flue gas stream. The percentage of CO_2 capture (φ) can be defined as a function of the molar flowrate of CO_2 in the flue gas ($Fg^0_{CO_2}$) and the molar flowrate of CO_2 in the vent gas ($Fg^h_{CO_2}$) :

$$\varphi = 1 - \frac{Fg^h_{CO_2}}{Fg^0_{CO_2}} \qquad (20)$$

In this work, this metric will be added as a constraint to ensure that the proposed absorber column design will meet a specific CO_2 capture target (CO_2*) in the presence of uncertainty, i.e.

$$\varphi_j(\mathbf{d}, \boldsymbol{\kappa}_j, \mathbf{x}_j, \mathbf{u}, \boldsymbol{\delta}_j) \geq CO_2^* \qquad \forall j = 1, 2, \ldots J \qquad (21)$$

As shown in (21), this inequality needs to be assessed for each realization considered in the uncertain parameters.

3.3 Results and discussion

The robust optimization formulation presented in the previous section was implemented in the Pyomo environment, an optimization library in PYTHON. The resulting set of differential and algebraic equations describing the absorber column model presented in section 3.1 was fully discretized using the backward finite-difference method. The interior-point optimization algorithm was used to search for local optimal solutions of the proposed robust optimization formulation presented in problem (18). The studies presented in this section were performed on an Intel Core i7-3770 CPU @ 3.4 GHz.

3.3.1 Model validation

In the present study, the data reported by Harun et al., (2011), which describes the behaviour of a pilot-scale CO_2 capture unit, was used to validate the implementation of the present absorption column model. A summary of the design parameters and base-case operating conditions used to perform the model validation are presented in Tables 1, 2 and 3. Note that the only constant physical properties used in the present model are those presented in Table 3. As discussed in section 3.1, the rest of the thermodynamic properties and kinetic parameters were estimated from correlations, which have been explicitly considered in the present column model, and therefore in the robust optimization formulation. To the authors' knowledge, this is the first study that performs robust optimization while using a detailed mechanistic process model for post-combustion CO_2 capture. As a result, the discretized absorption column model consisted on 6,963 nonlinear algebraic equations and 6,963 optimization (unknown) variables that were solved to local optimality in 1.6 s.

Table 1 Absorber column design and packing material

Packed column characteristic	
Column internal diameter (m)	0.43
Packing height (m)	6.1
Packing type	IMTP #40
Nominal packing size (m)	0.038
Specific area (m^2/m^3)	143.9

Table 2 Base case operating conditions, absorber column

Flue gas temperature (T_g^0)	319.71 K
Flue gas molar flowrate (F_g^0)	4.013 mol/s
Mole fraction	
CO_2	0.175
H_2O	0.025
MEA	0
N_2	0.8

Table 3 Constant physical properties

Properties	Source
T_{amb} = 297.6 K	Harun et al., (2011)
h_{out} = 430 W/m^{2}K	Kvamsdal and Rochelle (2008)
ΔH_{vap} = 48 kJ/mol	Reid et al., (1977)
ΔH_{rxn} = 82 kJ/mol	Kvamsdal and Rochelle (2008)
γ_{CO_2} = 0.381	Aspen Property Package
γ_{H_2O} = 0.974	Smith et al., (2005)
γ_{MEA} = 0.381	Smith et al., (2005)

Table 4 shows a comparison between the results obtained with the current model and those reported by Harun et al., (2011). The stream properties of the vent gas and the rich amine streams are used for validation (see Figure 3). As shown in Table 4, the vented gas contains a slightly larger amount of CO_2 than what was reported by Harun et al., (2011). However, the CO_2 vented meets the minimum requirements for the process to be acceptable. The composition of the other components in both streams are within acceptable limits. Also, the flowrates and outlet temperatures of the outlet streams are within 99% in agreement. Based on the above, the present

absorption column model is in reasonable agreement with the data reported in the literature and captures the behaviour of the post-combustion CO_2 capture absorption process.

Table 4 Model validation

	Vent gas stream		Rich amine stream	
	Current model	Harun et al., (2011)	Current model	Harun et al., (2011)
Temperature (K)	314.78	314.15	328.04	327.76
Total molar flow rate (mol/s)	3.53	3.47	31.68	30.51
Mole fraction				
CO_2	0.0108	0.0085	0.0502	0.0503
H_2O	0.0761	0.0651	0.8452	0.8475
MEA	0	0	0.1044	0.1021
N_2	0.9066	0.9264	0	0

3.3.2 Scenario A: Optimal process design

The aim of this scenario is to compare the design of the pilot-scale plant used to validate the present model (Harun et al., 2011) and that obtained from optimization. In the present analysis, all the thermodynamic, kinetic and operating parameters of the absorber column were assumed to be perfectly known, i.e. this scenario does not consider parameter uncertainty. Therefore, the formulation presented in (18) has been limited to one scenario (i.e. J=1).

Table 5 Base-case plant design and optimal plant design (Scenario A).

	Harun et al., (2011)	*Scenario A*
Decision variables		
Absorber diameter (m)	0.43	0.406
Absorber height (m)	6.1	5.9
Solvent flowrate (mol/s)	3.4	3.2
Capital costs ($/year)	572	247
Operating costs ($/year)	5,698	5,432
Total costs ($/year)	6,270	5,679

As shown in Table 5, the optimal design is 4% smaller than the original base-case design specification reported in Harun et al., (2011). The optimal MEA flowrate also decreases from the nominal condition. Similarly, a reduction of 5% in the overall costs of the column is observed. As shown in Table 5, almost 90% of the annualized total costs are due to the MEA consumption in the absorber unit, i.e. operating costs. This optimized design and operating condition meet the minimum CO_2 capture (CO_2*) required, which for the present scenario was set to 90%.

3.3.3 Scenario B: Uncertainty in flue gas stream

This scenario aims to search for the optimal design and operating conditions for the absorber column model under uncertainty. For this scenario, two key input parameters (i. e. , Fg_{CO_2} and Fg_{N_2}) were considered to be uncertain in order to approximate the best and worst scenario of flue gas concentration. These parameters are expected to change during operation due to sudden or scheduled changes in fossil-fired power plants. The robust optimization formulation presented in (18) was used to perform this study. For the present scenario, the CO_2 capture target rate (CO_2*) was set to 90%. The upper and lower bounds for the uncertain

parameters were set to 0.60 and 0.75 mol/s for Fg_{CO_2} and 3.21 and 3.1 mol/s for Fg_{N_2}. Also, the uncertain parameters were assumed to be uniformly distributed within their corresponding uncertain space domain; hence, $w_j = \frac{1}{J}$. One limitation of the proposed robust optimization formulation presented in problem (18) is that it highly depends on the number of uncertain realizations considered in the formulation. A limited number of realizations may return, in short computational times, solutions that may not be optimal or even inoperable for the entire range of space in the uncertain parameters set; conversely, an overly large number of realizations may improve the robustness of the design at the expense of significantly large or even prohibitive computational costs. In order to determine the minimum number of realizations needed to determine an optimal design and operating condition that remains operable (feasible) for the uncertain realizations in Fg_{CO_2} and Fg_{N_2}, the present scenario estimated the optimal design and operation of the absorption column under a different number of realizations in the uncertain parameters. That is, for each optimization run, the total number of realizations (J) was determined based on all the possible combinations between the individual realizations considered for each uncertain parameter.

Table 6 Optimal Steady-State Plant Design under uncertainty (Scenario B).

J=	100	81	64	49	36	25	16	9	4
Height (m)	6.023	6.023	6.010	6.001	5.998	5.998	5.998	5.987	5.986
Diameter (m)	0.410	0.410	0.410	0.410	0.410	0.410	0.410	0.410	0.409
Fl_{MEA} (mol/s)	3.21	3.21	3.209	3.209	3.209	3.209	3.2089	3.2089	3.208
CAP($/year)	253	253	253	252	252	252	252	252	252
OP ($/year)	5,447	5,447	5,446	5,446	5,446	5,447	5,446	5,446	5,444
Total ($/year)	5,700	5,700	5,698	5,698	5,698	5,698	5,698	5.697	5,696
CPU time (s)	154.53	93.08	62.36	42.80	26.07	16.37	11.46	5.71	3.41
Optimization variables	354,205	286,904	226,693	173,563	127,517	88,555	56,677	31,883	14,173
Number of equations and constraints	354,202	286,901	226,690	173,560	127,514	88,552	56,674	31,880	14,170

As shown in Table 6, for a short number of realizations, i.e., when the number of realizations (J) is between 4 and 25, the optimal operating conditions are 1% smaller than when a larger set of uncertainty is considered ($J \geq 81$). Additionally, larger computational times were obtained when a larger number of realizations was considered, i.e., the CPU time for J=81 is 96% more than that needed when J=4. These large differences in computational costs are a direct result of the size of the optimization problems considered, i.e. the number of equations and constraints when J=100 are 25 times more than that specified when J=4. As shown in Table 6, increasing J from 81 to 100 did not improve the quality of the solution but it increased the CPU costs by approximately 40%. Thus, the present analysis assumes that J=81 are sufficient to capture the absorber column's behaviour under uncertainty.

As discussed above, the results presented in Table 6 may indicate that differences in the process economics between the solutions found when using a small and large number of realizations are not significant (approximately 1%). However, these small changes in the design and operating conditions are critical and necessary to ensure feasibility and operability of the absorber column under a larger domain of uncertain scenarios.

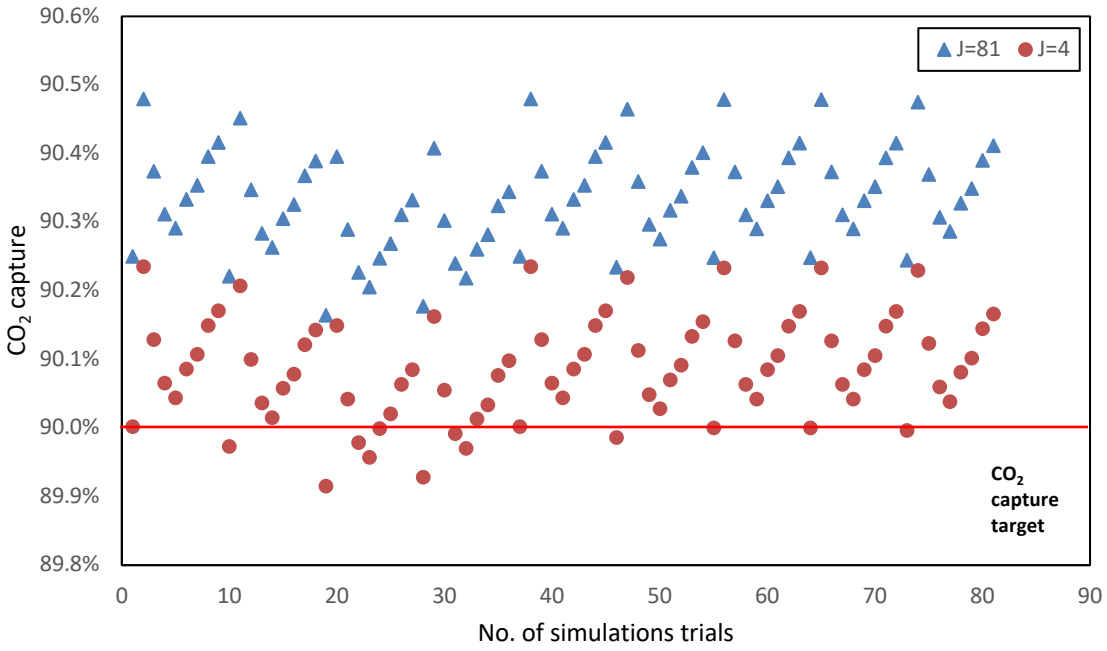

Figure 4 Effect of constraint violations under different uncertain horizon optimization

Figure 4 compares the performance of the two process designs obtained from J=4 and J=81 when multiple realizations in the uncertain parameters were randomly selected. As shown in this figure, over 10 violations of the CO_2* capture target constraint were observed when the optimal design and operating conditions specified by J=4 is employed. On the other hand, no constraint violations were observed when the design and operating conditions specified by J=81 were used. This result clearly demonstrates the impact of process uncertainty on the operability of the column and how small changes in the design and operating conditions can impact process performance.

3.3.4 Scenario C: Optimal design under different CO_2 capture rates

The aim of this scenario is to assess the impact different CO_2 capture rate levels have on the absorber column's design under uncertainty in the flue gas stream. As in *Scenario B*,

Fg_{CO_2} and Fg_{N_2} were considered as the uncertain parameters and under the same conditions. Thus, on the results presented in Table 6, 81 realizations in these uncertain parameters were considered for the present scenario. This scenario was evaluated under different CO_2 capture target levels (CO_2*) that spans from 89% to 95%.

Table 7 Optimal Steady-State Plant Design under uncertainty: Scenario C.

CO_2*	**89%**	**90%**	**92%**	**93%**	**94%**	**95%**
Height (m)	6.000	6.023	6.120	6.250	6.280	6.350
Diameter (m)	0.401	0.410	0.430	0.434	0.446	0.460
Fl_{MEA} (mol/s)	3.205	3.210	3.210	3.240	3.310	3.330
CAP($/year)	246	253	270	277	287	299
OP ($/year)	5,439	5,447	5,447	5,498	5,617	5,651
Total ($/year)	5,685	5,700	5,717	5,775	5,904	5,950

As shown in Table 7, the robust optimization formulation under uncertainty returned sizes and operating conditions for the column that are 9% and 3% larger when the minimum CO_2 capture rate level was increased from 89% to 95%, respectively. This demonstrates that process design and operating conditions are directly affected by the minimum CO_2 capture rate level. Therefore, the CO_2 target must be carefully chosen when specifying the optimal design for the absorber column. The results obtained from the present scenario were compared against the results obtained for *Scenario A* (no uncertainty considered) using the same CO_2 capture target levels (CO_2*) shown in Table 7. Figure 5 shows the total costs obtained from each scenario. In order to compensate uncertainty, larger dimensions of the absorber are observed for the robust optimization scenario. Conversely, a smaller design is specified for the case when no uncertainty is considered in the analysis (*Scenario A*). Furthermore, for a relatively low CO_2 capture rate level (i.e., CO_2* = 89%), the difference in the absorber costs between *Scenario A* and the present scenario is less than 1%. However, the difference in cost for a higher CO_2 capture target (CO_2* >

95%) can be up to 3% annually. This result indicates that uncertainty play a more significant role when higher CO_2 capture rate levels are specified. In addition, higher plant costs are expected when more stringent environmental constraints, e.g. high CO_2 capture rate levels, are considered when performing the optimal design of a CO_2 capture absorber unit under uncertainty.

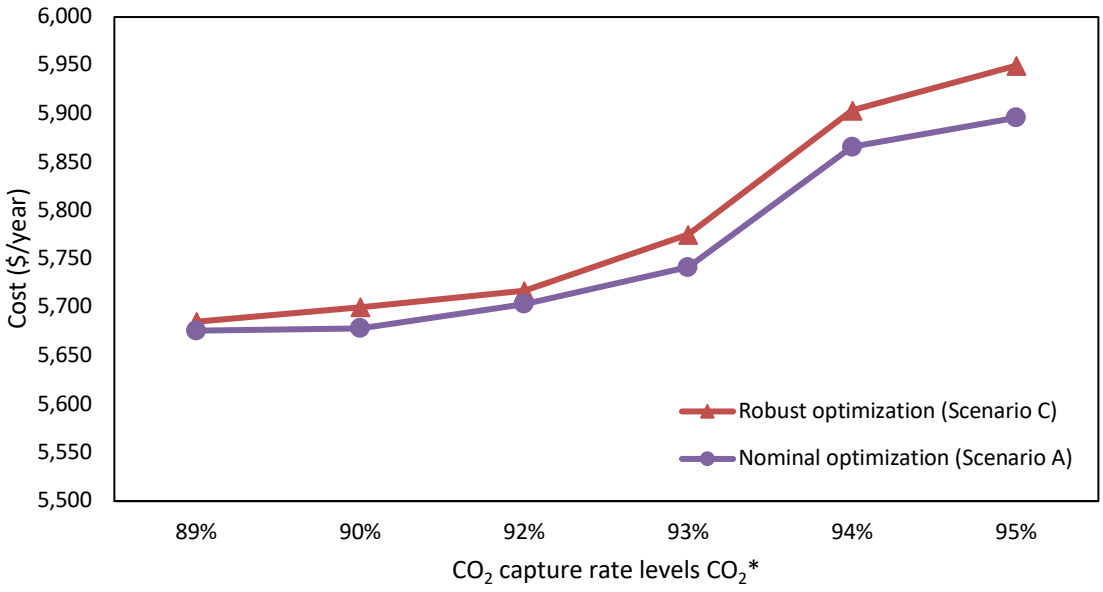

Figure 5 Economics of the absorber column under uncertainty in the flue gas stream.

3.3.5 Scenario D: Multiple process uncertainties

In this scenario, uncertainty was considered in three flue gas stream variables, i.e. flue gas flowrate of CO_2 and N_2 (Fg_{CO_2}, Fg_{N_2}) and temperature of the flue gas (Tg^0); in addition, uncertainty in the activity coefficient parameter (γ_{MEA}) in the gas-liquid interface was considered. Preliminary simulation studies showed that this parameter that has a significant effect on the system's pressure, as shown in equation (17). The upper and lower bounds for the uncertain parameters

were set to 0.6 and 0.76 mol/s for, 3.1 and 3.21 mol/s for, 316 and 319 K for T_g and 0.677 and 0.77 for γ_{MEA}. Also, the uncertain parameters were assumed to be uniformly distributed within their corresponding uncertain space domain; hence, $w_j = \frac{1}{J}$. As in *Scenario B*, a study on the number of realizations needed to accommodate the expected realizations in the uncertain parameters was conducted. For the present analysis, the minimum CO_2 capture rate level was set as to 90%.

Table 8 Optimal Steady-State Plant Design under uncertainty (Scenario D).

J	162	135	108	81	54	36	24
Height (m)	6.028	6.028	6.028	6.028	6.018	6.008	5.987
Diameter (m)	0.411	0.411	0.411	0.410	0.410	0.409	0.409
Fl_{MEA} (mol/s)	3.260	3.260	3.257	3.257	3.257	3.257	3.257
CAP($/year)	254	254	254	253	253	252	251
OP ($/year)	5,532	5,532	5,527	5,527	5,527	5,527	5,527
Total ($/year)	5,786	5,786	5,781	5,780	5,780	5,779	5,778
CPU time (s)	235.12	142.36	100.91	71.02	54.36	23.65	18.44

As shown in Table 8, a larger number of realizations were needed to obtain an optimal design and operating scheme that can accommodate all the expected realizations in the uncertain variables' space search. For the highest number of realizations (J=162), the optimal plant design for this scenario show sizes for both the column's height and diameter that are 2% higher than those reported for *Scenario A*. This increase in sizing is needed to accommodate the additional uncertain parameters considered in the present scenario. Similarly, larger computational demands are required for the present scenario since a significantly larger set of equations and variables need to be solved simultaneously. For instance, a total of 573,806 constraints and

573,809 variables are solved when J=162, which are 50% more equations than that required for *Scenario B* (J=81).

To further demonstrate the impact of parameter uncertainty on the absorber column's design, the optimal design and operating conditions obtained for *Scenario A* (i.e. no uncertainty in the formulation) were evaluated under different random realizations in the uncertain parameters considered for the present scenario.

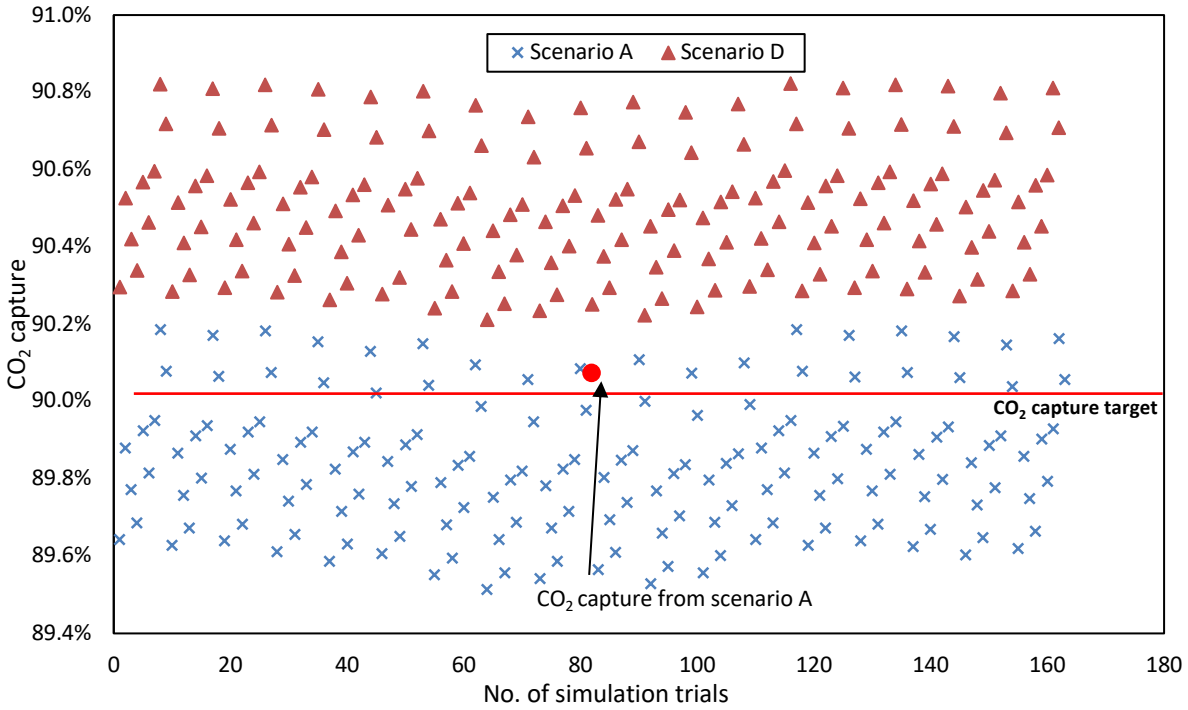

Figure 6 Effect of parameter uncertainty on Scenario A's design

As shown in Figure 6, *Scenario A*'s design is not able to comply with the minimum CO_2 capture rate level (90%) 80% of the time. Although the difference in sizes obtained from the present scenario and that obtained in Scenario A is not significant (i.e. approximately 2%), this result suggests that optimal design and operating conditions can fail to comply with process design goals if uncertainty is not explicitly modelled in the optimization formulation.

3.3.6 Scenario E: Uncertainty in solubility and additional process constraints

The aim of the present scenario is to consider additional uncertain parameters to those involved in Scenario D and to account for additional operational constraints that may impact the operation of the post-combustion unit. In the present analysis, the set of parameters that determine the solubility in the present adsorption column model were considered as uncertain parameters. These are the activity coefficient of CO_2, H_2O and MEA, i.e. γ_{H_2O}, γ_{CO_2} and γ_{MEA}. Note that the later was already considered as uncertain parameter in the previous scenario. Thus, a total of 6 uncertain parameters were involved in the present scenario. Moreover, two additional operational constraints were considered. The liquid-to-gas ratio L/G is considered to be an important operational parameter since it is related to process absorption capacity(Kvamsdal et al., 2009)(Kvamsdal et al., 2009)(Kvamsdal et al., 2009)(Kvamsdal et al., 2009)(Kvamsdal et al., 2009)(Kvamsdal et al., 2009)(Kvamsdal et al., 2009)(Kvamsdal et al., 2009)(Kvamsdal et al., 2009)(Kvamsdal et al., 2009). High L/G ratios are often required for this process to achieve acceptable CO_2 capture levels. In addition, this ratio also has a significant impact on the operability and design specifications of the absorber column (Kvamsdal et al., 2009). The liquid-to-gas ratio (L/G) can be defined as a function of the molar flowrate of the liquid phase (Fl) and the molar flowrate of the gas phase (Fg), i.e.

$$L/G=\frac{Fl}{Fg} \qquad (22)$$

In this study, a constraint of this ratio will be added to ensure that the proposed absorber column design will meet a specific L/G ratio (L/G*) in the presence of uncertainty, i.e.,

$$L/G\ (d, \kappa j, xj, u, \delta j) \geq L/G^* \qquad \forall j = 1, 2, \ldots J \qquad (23)$$

Moreover, effective mass transfer is another key factor for the absorption process. To this regard, the wetted surface area ($a_{g/l}$) (m^2/m^3) is key for development of effective mass transfer rates since it represents the specific gas-liquid interfacial area that is available for the mass transfer to occur. Hence, this variable is a dominant factor that impacts mass transfer operations in liquid-gas systems; the higher the value, the more mass transfer area available for absorption (Onda et al., 1968). Therefore, a constraint on a minimum wetted surface ($a_{g/l}*$) will be considered in the present scenario to ensure acceptable mass transfer operations under uncertainty, i.e.

$$a_{g/l}\ (d, \kappa j, xj, u, \delta j) \geq a_{g/l}* \qquad \forall j = 1, 2, \ldots J \qquad (24)$$

For the present analysis, L/G* and the $a_{g/l}*$ were set to 7 mol/mol and 130 m2/m3, respectively. Also, the minimum CO_2 capture rate level (CO_2*) was set to 90%. The upper and lower bounds for γ_{H_2O} were set to 0.877 and 1.071; similarly, upper and lower bounds for γ_{CO_2} were set to 0.343 and 0.420. The descriptions for the remaining uncertain parameters, i.e. Fg_{CO_2}, Fg_{N_2}, T_g^0 and γ_{MEA} remained the same as those specified in Scenario D. the resulting set of uncertain parameters were assumed to be uniformly distributed within their corresponding uncertain space domain; hence, $w_j = \frac{1}{J}$. Table 9 summarizes the results obtained for the present scenario. As shown in this table, larger equipment sizes were obtained for the present scenario when compared to Scenario D. Consequently, high annualized costs were obtained for this scenario; for example, the annualized costs for this scenario is 2% larger than that obtained for Scenario A. Given that two additional uncertain parameters are considered, a larger number of realizations were considered

for the present scenario (J=288), which is 43% larger than the maximum number of realizations considered in Scenario D (J=162). Accordingly, the resulting optimization problem involved a total of 1,032,192 equations and 1,032,195 variables, which are 45% more than that specified for Scenario D. Hence, the computational time required to obtain a solution for the present scenario increased 2 orders of magnitude when compared to that required by the optimization formulation specified for Scenario D. These results show that more real process designs involving multiple uncertain parameters and process operational constraints can be obtained with the proposed optimization formulation at the expense of higher computational costs.

Table 9 Optimal Plant Design (Scenario E)

J=	288
Height (m)	6.0301
Diameter (m)	0.421
Fl_{MEA} (mol/s)	3.262
CAP($/year)	261
OP ($/year)	5,536
Total ($/year)	5,796
CPU time (s)	482.3

Note that the original plant design used by Harun et al., (2012) (Table 5) is over specified for a CO_2 capture of 90%. Accordingly, the annualized costs of this over specified design are 14% larger when compared with the optimal design of the present scenario (Table 9).

3.4 Chapter Summary

The optimal process design of a CO_2 capture absorber column under uncertainty was presented. A robust optimization framework based on the multi-scenario approach was employed in this study to identify optimal design and operating schemes that comply with process operational constraints in the presence of uncertainty. Different scenarios were assessed in order to evaluate the impact of uncertainty on the optimal process design. In order to accommodate uncertainty, the process economics of the absorber column increases. This enlargement in the absorber specifications under robust optimization was greater for mores strict CO_2 capture policies, i.e., a higher CO_2 capture rate. Moreover, the differences in optimal design specifications in between different number of realizations may not be significant, however, the optimization under the right number of realizations is important in order to meet the environmental constraint of the process. However, the escalation in the annual costs may also lead to significant savings as this design will be able to comply with process constraints since uncertainty is explicitly considered in the process design stage calculation.

Chapter 4

Multi-objective Multi-period Optimization of a Post-combustion CO_2 Capture Absorber Column Under Uncertainty

The aim of this section is to present a study that considers multiple incentives while performing the optimal design and operations management of a CO_2 post-combustion absorption column. The central idea is to consider at the process design stage multiple variations that are expected to occur during plant operation such as seasonal changes in the power plant's demands as well as sudden or unexpected changes in the column's operation due to disturbances or uncertainty in the model parameters. In this chapter, a bi-objective optimization formulation was evaluated under uncertainty in the CO_2 flue gas composition and in physical and thermodynamic model parameters. In addition, a multi-scenario formulation is considered to account for the monthly changes in electricity demands in the province of Alberta, Canada in 2017 (AESO, 2017).

The organization of this chapter is as follows: the multi-period scenario for the CO_2 capture absorber column as well as the multi-objective formulation are described in section 4.1. Results from the proposed optimization formulations under uncertainty are presented and discussed in section 4.2. A summary of the results is presented in Section 4.3.

4.1 Introduction

Optimization under a single scenario where process inputs are assumed to remain constant during the entire period of operation may return inoperable or low economically attractive scenarios when these inputs change due to seasonal variations or sudden or unexpected disturbances. In order to determine optimal design and operations management conditions that

will be feasible under seasonal changes in the post-combustion CO_2 capture absorber, optimization should be evaluated under these variations. The operability of a post-combustion CO_2 capture process heavily relies on the changes that may be expected to occur in the inlet flue gas stream. Consequently, the flue gas stream coming from a combustion process from a power plant mainly depends on the energy demands and production which may change seasonally. In order to account for that condition, multiple scenarios representing monthly average energy loads will be considered in the present formulation. This work assumes that these changes in energy demands are directly proportional to the expected seasonal changes in the power plant's flue gas stream.

Canada is listed as one of the ten countries with the highest CO_2 emissions worldwide with almost 11% of those emissions are produced from electricity generation (Boden et al., 2017; UNFCCC, 2018; BP, 2018; National Energy Board, 2017). According to the National Energy Board, (2017), the Canadian province with more greenhouse gas intensity of electricity generation is Alberta. Furthermore, approximately 87% of the electricity in Alberta is produced from fossil fuels – approximately 47% from coal and 40% from natural gas. The remaining 13% is produced from renewables, such as wind, hydro, and biomass (National Energy Board, 2017). Since more than half of electricity in Alberta is produced by the combustion of fossil fuels, a scenario of monthly average energy loads in Alberta will be considered in this work. Moreover, the monthly energy loads will be assumed to be directly proportional to seasonal changes expected in the operation of a CO_2 capture plant. The monthly profile of the energy load in the province of Alberta in the year 2017 is illustrated in Figure 7. The column absorption model described in Chapter 3.1 was evaluated for 12 periods with each period representing a month of the year. In order to account for the energy load variations in the present multi-period study for the CO_2 capture plant, the variability in the flue gas flow-rate were proportionally adjusted with respect to that observed in

the monthly energy loads in the province of Alberta, i.e.

$$Fg_p^0 = \left(\frac{EL_p}{\overline{EL}}\right) Fg^0 \qquad (25)$$

where $\overline{EL}$ represents the mean annual energy load in the province of Alberta estimated from data reported in the open literature and shown in Figure 7 (9,393 MW) whereas Fg^0 represents the mean flue gas flow rate considered in the present study for the CO_2 capture plant. This value was obtained from data reported in the literature (see Table 2). EL_p represents the monthly energy load in the period p whereas Fg_p^0 represents the monthly flue gas flowrate considered in each period p. The resulting multi-period scenario of the absorber column where each period of time had a different flue gas stream proportional to the seasonal energy load is shown Figure 7.

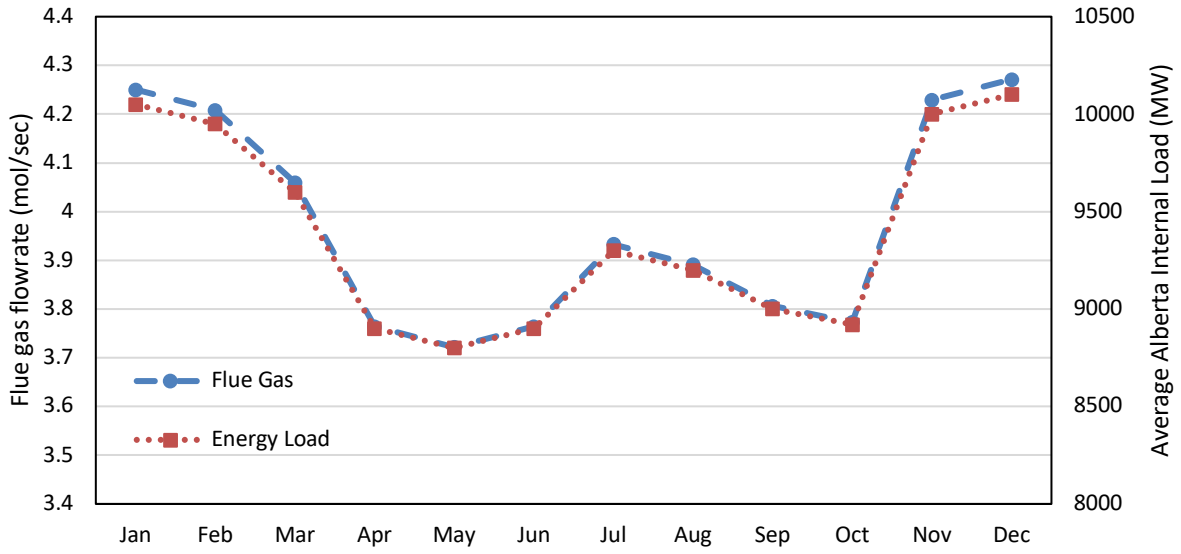

Figure 7 Monthly average load in 2017 (AESO, 2017)

This multi-period scenario aims to approximate real power plant's behaviour under this type of seasonal changes in the flue gas stream. Moreover, the multi-period scenario will also consider

input and model parameter uncertainty to consider a more realistic condition of a real post-combustion CO_2 capture process during operation. Furthermore, this study will seek for the optimal process design and operations management conditions of the CO_2 capture absorber process under two conflicting objectives. That is, the present multi-scenario analysis described above will be evaluated under a multi-objective optimization framework that will explicitly consider uncertainty in the CO_2 absorber unit. This optimization framework will most surely guarantee that the proposed solutions will accommodate the possible scenarios that a real-life process can experience. To the author's knowledge, studies similar to that considered in this work have not been presented in the open literature.

4.1.1 Mathematical Framework

This section presents the conceptual formulation of the multi-objective multi-scenario optimization under uncertainty. The two objective functions that were considered for the present formulation are: minimization of the capital and operating costs of the absorber column and maximization of the CO_2 capture of the absorber tower. Since the single absorber unit has been considered under this study, these two objectives are the most appropriate functions in the decision to determine the optimal design for the absorber unit because of their impact and implications in post-combustion CO_2 capture plants. The bi-objective multi-period optimization formulation considered is explicitly described as a function of the uncertainty in the process. Hence, the conceptual mathematical formulation considered in this study is as follows:

$$\max_{\mathbf{d},\mathbf{u_p}} \; f_1 = \sum_{j=1}^{J} w_j \left(\Theta_{max}\left(\mathbf{d}, \boldsymbol{\kappa}_{\mathrm{j,p}}, \mathbf{x}_{\mathrm{j,p}}, \dot{\mathbf{x}}_{\mathrm{j,p}}, \mathbf{u}_{\mathrm{p}}, \boldsymbol{\delta}_{\mathrm{j,p}}\right) \right)$$

$$\min_{\mathbf{d},\mathbf{u_p}} \; f_2 = \sum_{j=1}^{J} w_j \left(\Theta_{min}\left(\mathbf{d}, \boldsymbol{\kappa}_{\mathrm{j,p}}, \mathbf{x}_{\mathrm{j,p}}, \dot{\mathbf{x}}_{\mathrm{j,p}}, \mathbf{u}_{\mathrm{p}}, \boldsymbol{\delta}_{\mathrm{j,p}}\right)\right)$$

s.t.

$$g\ (\mathbf{d}, \boldsymbol{\kappa}_{\mathrm{j,p}}, \dot{\mathbf{x}}_{\mathrm{j,p}}, \mathbf{x}_{\mathrm{j,p}}, \mathbf{u}_{\mathrm{p}}, \boldsymbol{\delta}_{\mathrm{j,p}}) = 0, \qquad \forall \mathrm{j} = 1, 2, \ldots \mathrm{J} \quad \forall \mathrm{p} = 1, 2, \ldots \mathrm{P}$$

$$h\ (\mathbf{d}, \boldsymbol{\kappa}_{\mathrm{j,p}}, \dot{\mathbf{x}}_{\mathrm{j,p}}, \mathbf{x}_{\mathrm{j,p}}, \mathbf{u}_{\mathrm{p}}, \boldsymbol{\delta}_{\mathrm{j,p}}) \geq 0, \qquad \forall \mathrm{j} = 1, 2, \ldots \mathrm{J} \quad \forall \mathrm{p} = 1, 2, \ldots \mathrm{P}$$

$$\mathbf{d}^{\mathrm{l}} \leq \mathbf{d} \leq \mathbf{d}^{\mathrm{u}}$$

$$\mathbf{u}_{\mathrm{p}}{}^{\mathrm{l}} \leq \mathbf{u}_{\mathrm{p}} \leq \mathbf{u}_{\mathrm{p}}{}^{\mathrm{u}} \qquad (26)$$

where g is the equality constraints representing the complete mechanistic absorption column's model presented in Equations (6) to (17). Moreover, h represents the operational or environmental inequality constrains considered in the formulation. Similarly, $\mathbf{d}$ is the process design variables, $\boldsymbol{\kappa}$ represents the model parameters, $\mathbf{x}$ represents the state variables (i.e., molar concentrations of each component or temperature of gas or liquid phase) whereas $\dot{\mathbf{x}}$ represent the changes of the process state variables with respect to the axial domain (z). The operating variables that can be adjusted during operation are denoted by $\mathbf{u}$ whereas $\boldsymbol{\delta}$ represents the set of uncertain parameters considered in the optimization formulation. Moreover, w_j represents a weight assigned for each realization j in the uncertain parameters, i.e., $\sum_{j=1}^{J} w_j = 1$. These weights may be estimated using a probabilistic distribution function for the uncertain parameters that is known a priori from process experience or experimental observations. The term J represents the set of discrete realizations or scenarios considered for the uncertain model parameters; accordingly, the cost function ($\Theta_{min}, \Theta_{max}$), the process model equations and constraints (i.e. g and h) are described for each realization (j) considered for the uncertain parameter set $\boldsymbol{\delta}$. Moreover, the index p represents the time-periods considered in the formulation.

The decision variables considered for the bi-objective optimization are the height and diameter of the absorber column (i.e. H_{abs} and D_{abs}) which are the main process design parameters **d** in the absorber column. Similarly, the inlet flowrate (Fl_{MEA}) is assumed to be a variable that can be adjusted during operation, i.e. during each period *p*; accordingly, this variable is represented as $\mathbf{u}_p$.

The minimization cost function considered in the present analysis is the same correlation considered in economic cost function in Equation (27). However, the operating cost will now be considered to be in function of the periods *p*, i.e.

$$\Theta_{min} = A * ROR\left(\frac{CEPCI}{B}\right) D_{abs}^{1.06} H_{abs}^{0.82} + \sum_{p=1}^{P} w_p (Fl_{MEA,p} C_{MEA}) \qquad (27)$$

where w_p represents a weight assigned for each period *p*. In the present study, the rate of CO_2 capture ($\varphi_{j,p}$) will be estimated for every period (*p*) and every uncertain realization (*j*). As shown in (27), this variable is a function of the molar flowrate of CO_2 in the flue gas ($Fg^{0}_{CO_2,j,p}$) and the molar flowrate of CO_2 in the vent gas ($Fg^{h}_{CO_2,j,p}$).

$$\varphi_{j,p} = \left(1 - \frac{Fg^{h}_{CO_2,j,p}}{Fg^{0}_{CO_2,j,p}}\right) \times 100 \qquad \forall j = 1, 2, \dots J \qquad \forall p = 1, 2, \dots P \qquad (28)$$

Thus, $\varphi_{j,p}$ is used here to specify an environmental constraint that enforces a minimum CO_2 capture target (CO_2*) that the proposed absorber column design is required to satisfy for every uncertain realization *j* and period *p* , i.e.

$$\varphi_{j,p}\,(\mathbf{d}, \boldsymbol{\kappa}_{j,p}, \mathbf{x}_{j,p}, \mathbf{u}_p, \boldsymbol{\delta}_{j,p}) \geq CO_2^* \qquad \forall j = 1, 2, \dots J \qquad \forall p = 1, 2, \dots P \qquad (29)$$

While a CO_2 capture target constraint is needed to ensure that this environmental constraint meets a minimum threshold during operation; it may also be needed to maximize the overall rate of CO_2 captured on an annual basis such that the design goals of post-combustion CO_2 capture plants may be satisfied. Therefore, in addition to ensuring a minimum CO_2 capture rate for every *j* and *p* as shown in (29), the present study aims to maximize the CO_2 capture rate ($\varphi_{j,p}$) at every period of operation of the absorber column, and for every realization in the uncertain parameters, i.e.

$$\Theta_{max} = \sum_{p=1}^{P} w_p \left(\sum_{j=1}^{J} \varphi_{j,p}\right) \qquad \forall j = 1, 2, \dots J \qquad \forall p = 1, 2, \dots P \qquad (30)$$

Based on the above, the present formulation involves two objective functions shown in equations (27) and (30), which are usually conflicting in nature. In order to determine the optimal solution of a multi-objective problem, a specific solution strategy must be deployed. Given that the bi-objective optimization methods described in section 2.4.2. provide a direct solution to multi-objective formulations; these methods were considered to solve the present multi-objective optimization problem. First, the optimal design and operations management for the absorber column between the two objectives shown in equations (27) and (30) was estimated using the 1NM method described in equation (3). The trade-off surface or Pareto front was generated to validate the solution from the 1NM method. The corresponding trade off surfaces were calculated using the ε-constraint method illustrated in section 2.4.2 and shown in Equation (2). Based on the above, problem (26) can be reformulated in terms of the ε-constrained method and 1NM method as follows:

- ε-constraint method

$$\underset{\mathbf{d},\mathbf{u}_p}{\text{Minimize}} \; f_{2\_CC} = \sum_{j=1}^{J} w_j \left(\Theta_{min}\left(\mathbf{d}, \boldsymbol{\kappa}_{j,p}, \mathbf{x}_{j,p}, \dot{\mathbf{x}}_{j,p}, \mathbf{u}_p, \boldsymbol{\delta}_{j,p}\right) \right)$$

s.t.

$$\Theta_{max}\left(\mathbf{d}, \boldsymbol{\kappa}_{j,p}, \mathbf{x}_{j,p}, \dot{\mathbf{x}}_{j,p}, \mathbf{u}_p, \boldsymbol{\delta}_{j,p}\right) \leq \varepsilon \qquad \forall j = 1, 2, \dots J \quad \forall p = 1, 2, \dots P$$

$$h(\mathbf{d}, \boldsymbol{\kappa}_{j,p}, \dot{\mathbf{x}}_{j,p}, \mathbf{x}_{j,p}, \mathbf{u}_p, \boldsymbol{\delta}_{j,p}) \geq CO_2^* \qquad \forall j = 1, 2, \dots J \quad \forall p = 1, 2, \dots P$$

$$g(\mathbf{d}, \boldsymbol{\kappa}_{j,p}, \dot{\mathbf{x}}_{j,p}, \mathbf{x}_{j,p}, \mathbf{u}_p, \boldsymbol{\delta}_{j,p}) = 0 \qquad \forall j = 1, 2, \dots J \quad \forall p = 1, 2, \dots P$$

$$\mathbf{d}^l \leq \mathbf{d} \leq \mathbf{d}^u$$

$$\mathbf{u}_p{}^l \leq \mathbf{u}_p \leq \mathbf{u}_p{}^u \qquad (31)$$

- 1NM method:

$$\underset{\mathbf{d},\mathbf{u}_p}{\text{Minimize}} \quad \left(1 - \widehat{f_{1_{CO_2}}}(\mathbf{d}, \boldsymbol{\kappa}_{j,p}, \mathbf{x}_{j,p}, \dot{\mathbf{x}}_{j,p}, \mathbf{u}_p, \boldsymbol{\delta}_{j,p})\right) + \widehat{f_{2_{CC}}}(\mathbf{d}, \boldsymbol{\kappa}_{j,p}, \mathbf{x}_{j,p}, \dot{\mathbf{x}}_{j,p}, \mathbf{u}_p, \boldsymbol{\delta}_{j,p})$$

s.t.

$$g(\mathbf{d}, \boldsymbol{\kappa}_{j,p}, \dot{\mathbf{x}}_{j,p}, \mathbf{x}_{j,p}, \mathbf{u}_p, \boldsymbol{\delta}_{j,p}) = 0 \qquad \forall j = 1, 2, \dots J \quad \forall p = 1, 2, \dots P$$

$$h(\mathbf{d}, \boldsymbol{\kappa}_{j,p}, \dot{\mathbf{x}}_{j,p}, \mathbf{x}_{j,p}, \mathbf{u}_p, \boldsymbol{\delta}_{j,p}) \geq CO_2^* \qquad \forall j = 1, 2, \dots J \quad \forall p = 1, 2, \dots P$$

$$\mathbf{d}^l \leq \mathbf{d} \leq \mathbf{d}^u$$

$$\mathbf{u}_p{}^l \leq \mathbf{u}_p \leq \mathbf{u}_p{}^u \qquad (32)$$

where:

$$\widehat{f_{1\_CO_2}}\left(\mathbf{d}, \boldsymbol{\kappa}_{j,p}, \mathbf{x}_{j,p}, \dot{\mathbf{x}}_{j,p}, \mathbf{u}_p, \boldsymbol{\delta}_{j,p}\right) = \frac{f_{1\_CO_2}\left(\mathbf{d}, \boldsymbol{\kappa}_{j,p}, \mathbf{x}_{j,p}, \dot{\mathbf{x}}_{j,p}, \mathbf{u}_p, \boldsymbol{\delta}_{j,p}\right) - LB\left(f_{1\_CO_2}\right)}{UB\left(f_{1\_CO_2}\right) - LB\left(f_{1\_CO_2}\right)}; \quad \forall j = 1, 2, \dots J \quad \forall p = 1, 2, \dots P$$

$$\widehat{f_{2\_CC}}\left(\mathbf{d}, \boldsymbol{\kappa}_{j,p}, \mathbf{x}_{j,p}, \dot{\mathbf{x}}_{j,p}, \mathbf{u}_p, \boldsymbol{\delta}_{j,p}\right) = \frac{f_{2\_CC}\left(\mathbf{d}, \boldsymbol{\kappa}_{j,p}, \mathbf{x}_{j,p}, \dot{\mathbf{x}}_{j,p}, \mathbf{u}_p, \boldsymbol{\delta}_{j,p}\right) - LB\left(f_{2\_CC}\right)}{UB\left(f_{2\_CC}\right) - LB\left(f_{2\_CC}\right)}; \quad \forall j = 1, 2, \dots J \quad \forall p = 1, 2, \dots P$$

(33)

where UB ($f_{1\_CO_2}$) and LB (f_{2_CC}) are the values of $f_{1\_CO_2}$ and f_{2_CC} when optimized respectively, over the constraint set; similarly, $\widehat{f_{1\_CO_2}}$ and $\widehat{f_{2\_CC}}$ are the normalized functions of $f_{1\_CO_2}$ and f_{2_CC}, respectively. In addition, $f_{1\_CO_2}$ represents the CO_2 capture rate function to be maximized given by equation (30) whereas f_{2_CC} represents the capital and operating costs function that will be minimized and that is shown in Equation (27).

4.2 Results and discussion

The multi-objective optimization formulation presented in the previous section was implemented in the Pyomo environment, an optimization library in PYTHON. The resulting set of differential and algebraic equations describing the absorber column model presented in Equations (6) to (16) in a multi-period scenario were fully discretized using the backward finite difference method. The interior-point optimization algorithm was used to search for local optimal solutions of the proposed robust optimization formulation presented in problems (31)-(32). The studies presented in this section were performed on an Intel Core i7-3770 CPU @ 3.4 GHz. The proposed multi-objective multi-period formulations shown in (28)-(29) were solved under different scenarios, which are discussed next.

4.2.1 Scenario A: Single period multi-objective optimization

The first scenario considers a multi-objective design optimization of the post-combustion CO_2 capture absorber under a single period scenario. The model parameters and process specifications presented in Tables 1, 2 and 3 in Section 3.3.1 were used in the present

formulation. Moreover, the present scenario assumes that all the model parameters and inputs remain constant and equal to a nominal value. Therefore, the formulation presented in problem (31)-(32) has been limited to one scenario and one period (i.e. J=1, P=1). For the 1NM optimization method the minimum CO_2 capture (CO_2*) was set to 85%.

In order to determine if the 1NM optimal result was a suitable trade-off solution, the Pareto surface was constructed under the ε-constraint formulation presented (31).

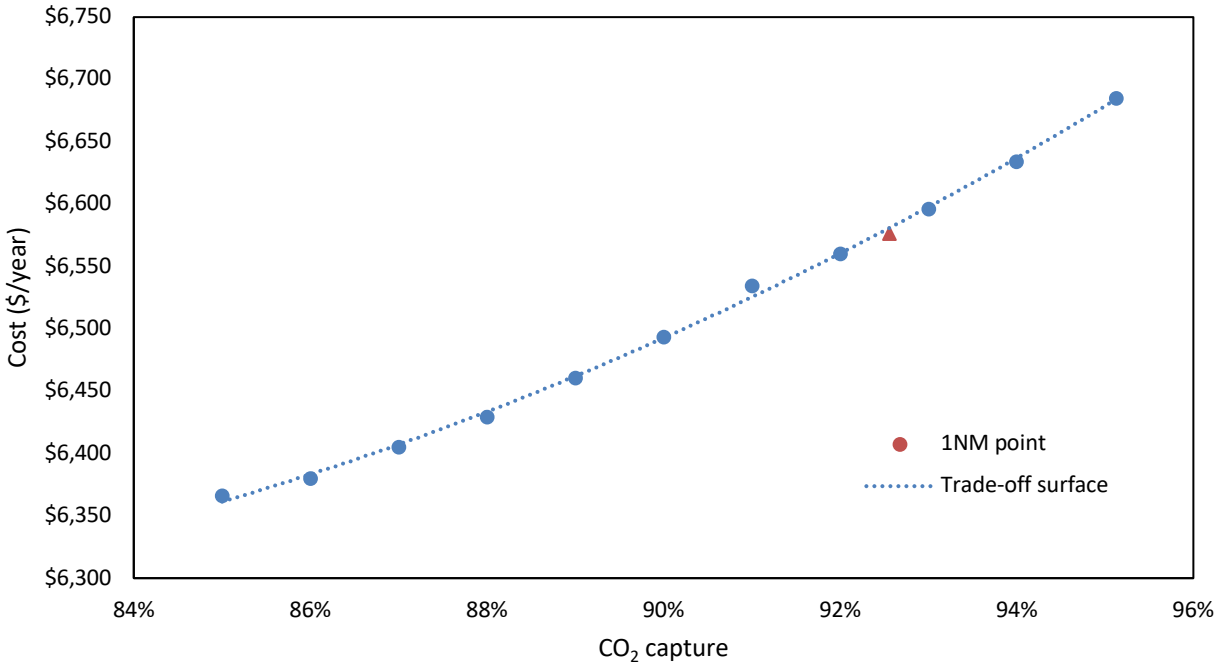

Figure 8 Single period trade-off surface

Figure 8 shows the 1NM solution point and the trade-off or Pareto surface of the bi-objective results of this scenario. In order to build the Pareto surface, optimization was carried out under ε-constraint bi-optimization, ε was subjected to CO_2 capture target levels constraint. Likewise,

the optimized designs and operating conditions obtained for each ε problem were solved under the same CO_2 capture (CO_2*) rate (i.e. 85%).

The upper bound of the Pareto surface was determined by optimizing exclusively equation (30), whereas the lower bound was obtained from the solution of Equation (27). Between the upper and lower bounds, 9 uniformly distributed points were used to build the Pareto surface; this number of pareto points was needed to generate a smooth Pareto surface, as shown in Figure 8. A total of 5,238 constraints and 5,239 variables were generated for each ε-constraint optimization problem with an average CPU solution time of 9.05 seconds. On the other hand, the 1NM optimization produced an optimization problem with 5,237 constraints and 5,239 variables that was solved in 2.19 seconds (CPU time). Note that the additional constraint in the former method involves the ε-constraint that limits the CO_2 capture rate as shown in equation (31). Figure 8 shows that the trade-off surface follows a linear behaviour of the Pareto optimal points. Moreover, this figure also shows that the optimal trade-off point obtained from the 1NM method lies near the trade-off surface. Table 9 shows the design parameters obtained from the 1NM bi-objective optimization calculation. As shown in this table, a high CO_2 capture rate was obtained as the optimal solution of the upper bound; however, this target also shows the highest annual costs for this process. The opposite was observed for the lower bound solution. On the other hand, the 1NM point presents a suitable trade-off solution. That is, the CO_2 capture from the 1NM point is only 2.71% smaller than the upper bound and 8.8% larger than the lower bound CO_2 capture. Similarly, the annualized costs reflect an increase in the design specifications for the upper bound, where it is 2% more expensive to operate the plant at the maximum CO_2 capture target than at the optimal 1NM design.

Table 10 Scenario A: Multi-objective design specifications

	Lower Bound	Upper Bound	1NM point
Height (m)	5.50	6.35	6.15
Diameter (m)	0.38	0.456	0.43
MEA flowrate (mol/sec)	3.23	3.23	3.23
Capital Cost ($/year)	885	1,204	1,097
Operating Cost ($/year)	5,481	5,481	5,480
Θ_{min} [Annual Cost ($/year)]	6,366	6,685	6,577
Θ_{max} [% CO_2 capture]	85 %	95.13 %	92.55 %

4.2.2 Scenario B: Multi-objective multi-period optimization

The aim of this scenario was to determine the optimal design and operating conditions under seasonal changes in the operation of the absorber tower. Accordingly, the fluctuations in the flue gas flowrate described in Figure 7 were considered using the multi-objective multi-period formulation presented in problems (31)-(31). As in the previous scenario, all the model parameters of the absorber column were assumed to be perfectly know, i.e. uncertainty is not considered in the present scenario. Thus, the formulation presented in problems (31)-(32) has been limited to one scenario and twelve periods (i.e., J=1, P=12). Also, the periods were assumed to be uniformly distributed within their corresponding period, i.e. $w_p = \frac{1}{P}$. The minimum CO_2 capture (CO_2*) were defined as in Scenario A, i.e. CO_2*=85%.

A total of 96,954 variables and 96,967 constraints were evaluated with an average CPU time of 82.51 seconds for each instance under the ε-constraint method whereas the 1NM method generated problems with 96,954 variables and 96,954 constraints that required a CPU time of 63.07 seconds.

Figure 9 shows the Pareto solutions of the present scenario as well as the 1NM optimal point. Between the upper and lower bounds, 8 uniformly distributed points were required to build a smooth Pareto surface. Figure 9 shows that the optimal trade-off 1NM point is not trivial since it does not lie at the mid-point of the Pareto front surface.

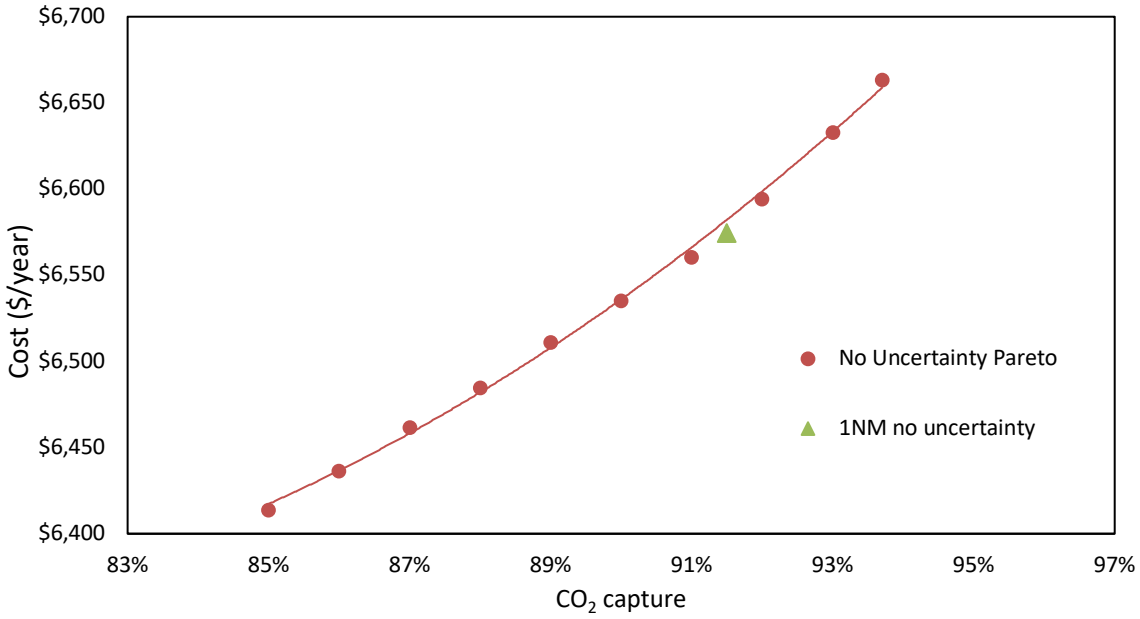

Figure 9 Trade-off surface for multi-period scenario at nominal conditions (J=1, P=12)

Table 10 shows the design specifications obtained from the multi-period 1NM bi-objective optimization. In order to compensate for the changes in the flue gas flowrate during the multi-period scenario, a reduction of 1.5% in the CO_2 capture is obtained as the upper bound of the trade-off surface when compared to the upper bound of CO_2 capture presented in Scenario A (Table 11). This reduction in the upper bound for the multi-period scenario leads to a slightly smaller CO_2 capture rate and process design (approximately 1 % in both diameter and height)

from the 1NM point compared to the 1NM solution obtained from Scenario A. Although a smaller optimal CO_2 capture is observed in this scenario than in scenario A, these results consider a more realistic operation since they account for seasonal fluctuations in the flue gas flowrate.

Table 11 Scenario B: Multi-period Multi-objective design specifications

	Lower Bound	Upper Bound	1NM point
Height (m)	5.77	6.34	6.09
Diameter (m)	0.38	0.45	0.428
Capital Cost ($/year)	933	1,182	1,095
Operating Cost ($/year)	5,481	5,481	5,479
Θ_{min} [Annual Cost ($/year)]	6,414	6,663	6,575
Θ_{max} [% CO_2 capture]	85 %	93.70 %	91.52 %

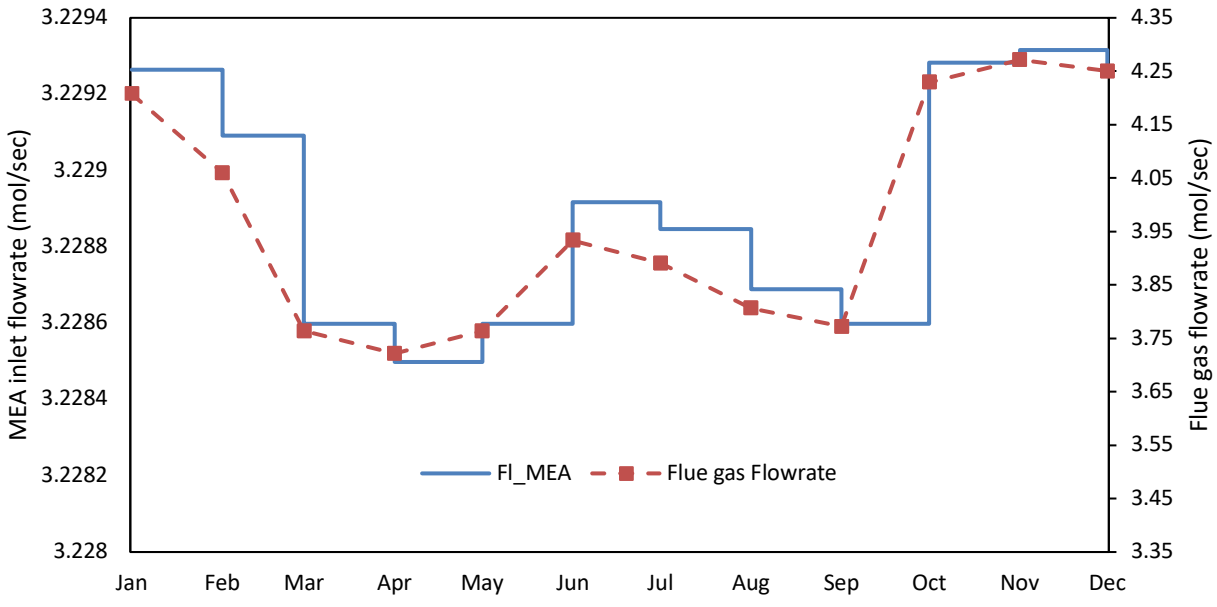

Figure 10 MEA inlet flowrate profile for multi-period optimization

Figure 10 illustrates the profile in the MEA flowrate obtained under the 1NM point optimal design specifications. This profile is compared against periodical changes in the flue gas mass flowrate. As shown in this Figure 10, there is a direct correlation between MEA consumption and flue gas flow rate, e.g. less MEA is required when there is a decrease in the flue gas flow rate.

Figure 11 shows the periodic changes in the CO_2 capture rate related to the changes in flue gas flow rate. As shown in this figure, the 1NM solution point is able to maintain a low MEA flowrate and relatively high CO_2 capture rate when less flue gas is fed to the absorber column. This confirms that the 1NM solution point is indeed a trade-off solution since it balances annual costs (reflected in the MEA consumption) and CO_2 emissions.

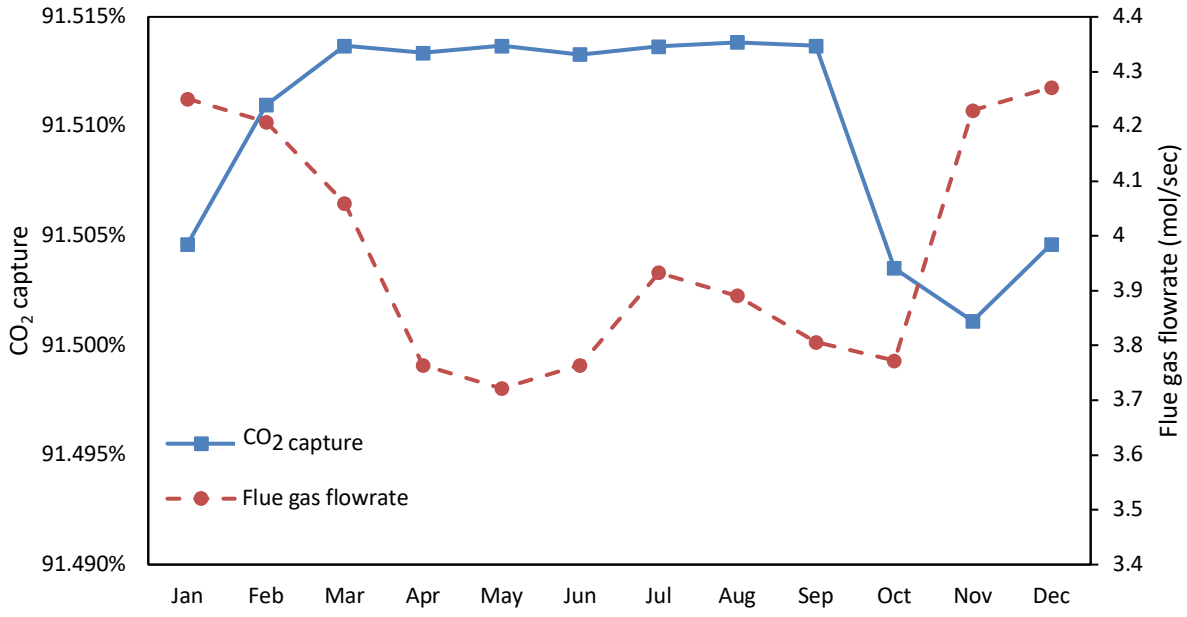

Figure 11 CO_2 capture profile for multi-period optimization

Moreover, 1NM design specifications from Scenario B were simulated maintaining a constant mean value of the MEA flowrate obtained from the 1NM solution point. Figure 12 illustrates how this constant MEA flowrate will perform along the seasonal changes affecting the CO_2 capture.

The average of CO_2 capture rate obtained from this simulation (91.50%) is slightly smaller than that obtained when periodic changes in MEA flowrate are considered (91.51%). However, the standard deviation (i.e. the variability) in the CO_2 capture rate for the case of a constant (mean) MEA flowrate shown in Figure 12 is 40% larger than that obtained when the MEA flowrate is adjusted for each period (Figure 11). These results indicate the need to adjust the MEA flowrate according to the flue gas stream conditions to improve the operability and economics of this process.

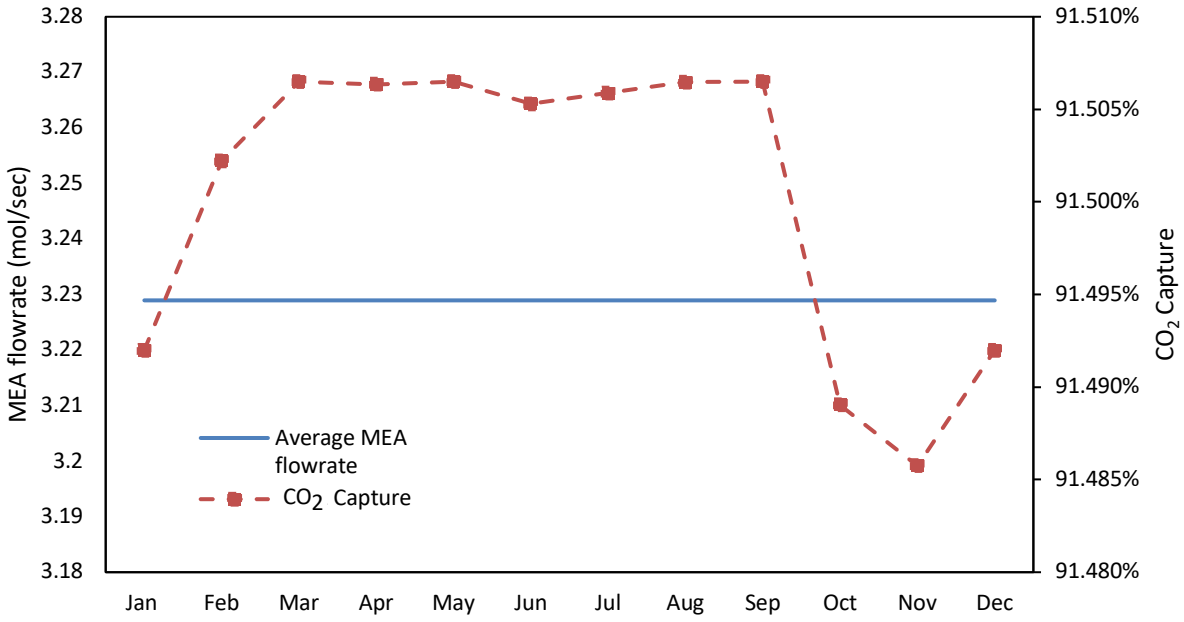

Figure 12 CO_2 Capture profile with constant MEA flowrate

4.2.3 Scenario C: Multi-objective multi-period optimization under uncertainty

In this scenario, uncertainty was considered in the flue gas composition of the CO_2 (y_{CO_2}), in the equilibrium pressure parameter (γ_{MEA}) and in the heat of reaction (ΔH_{rxn}). The upper and lower bounds for these uncertain parameters were set to 0.667 and 0.677 for γ_{MEA}, -8,0000 and -8,4000 for ΔH_{rxn} and 0.12 and 0.19 for y_{CO_2}, respectively. Also, the uncertain parameters were assumed to be uniformly distributed within their corresponding uncertain space domain, i.e. $w_j = \frac{1}{J}$. The number of realizations J was determined based on a balance between the range of space in the uncertain parameters and computational costs. The objective of this scenario is to evaluate the multi-period scenario for a multi-objective optimization under process uncertainty and seasonal changes in the flue gas flowrate, an aspect that has never been previously studied for this process. A total of 16 uncertain scenarios (J=16) and 12 periods (P=12) where considered in the analysis. As in Scenario B, the periods were assumed to be uniformly distributed within their corresponding space domain, i.e. $w_p = \frac{1}{P}$. The optimization technique was the same used for the previous scenarios, i.e., 1NM method to obtain the optimal design under bi-objective problem and ε-constraint method to build the trade-off surface. CO_2 capture constraints were set as stated in the previous scenario, i.e. the minimum CO_2 capture (CO_2*) was set to 85%.

The ε-constraint optimization problems consisted of a total of 604,595 variables and 604,996 constraints that were solved in an average CPU time of 4,688 seconds. Similarly, the 1NM optimization problem involved 604,595 variables and 604,788 constraints that were solved in a CPU time of 2,130 seconds. As a result of the additional constraints considered in the ε-constraint problems due to the multiple uncertainty realizations considered in this scenario, higher computational times were observed for this solution method. Moreover, the number of

uncertainty realizations under a multi period scenario will impact the computational costs. For the ε-constraint method, the CPU times reported for the present scenario are approximately 972 and 34 times higher than those obtained for scenario A and scenario B, respectively. Similarly, the CPU times reported for the 1NM method are 518 and 57 higher than those observed for Scenario A and B, respectively.

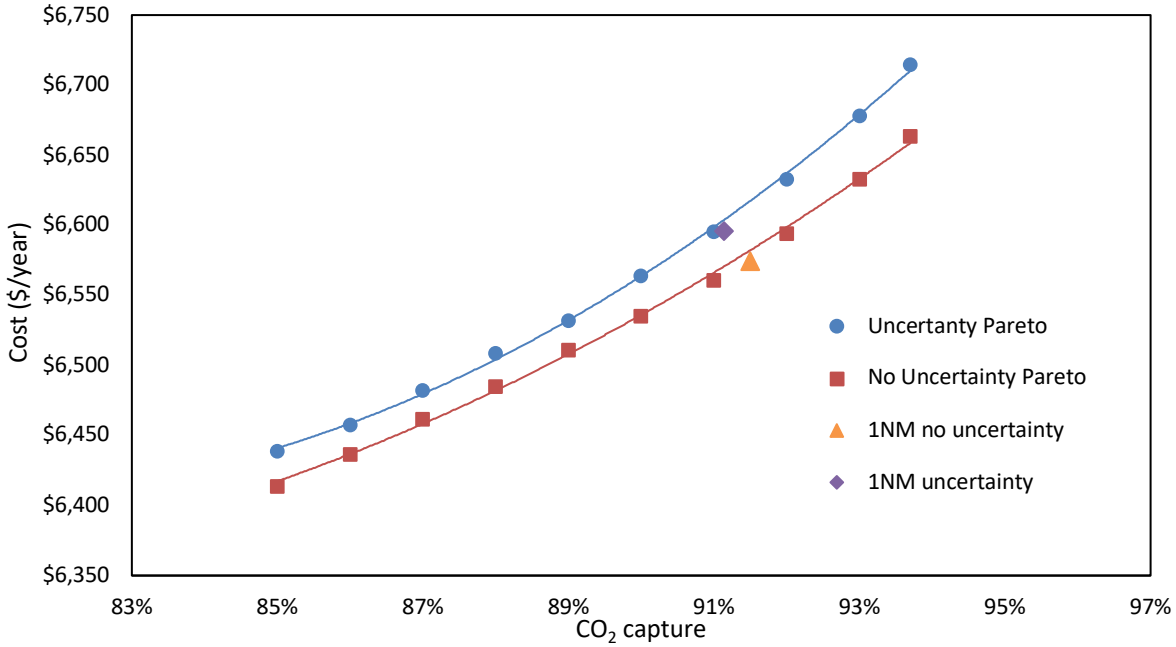

Figure 13 Comparison of Scenarios B and C

Figure 13 shows a comparison between the Trade-off solutions under nominal conditions (J=1) and under uncertainty (J=16). Hence, optimal Pareto points for optimization under uncertainty show larger annualized costs compared to the Pareto optimal points for nominal conditions in an order of 0.5 - 1%. Likewise, optimal 1NM point under uncertainty showed a slight increase of 0.3% in the annualized costs compared to those reported for the nominal case (Scenario B). Table 12 presents the design specifications and annual costs of the bi-objective optimization under

uncertainty using the 1NM method. As shown in Table 12, the optimal CO_2 capture rate is smaller than that obtained for scenario B giving a value of 91.16% CO_2 capture, this reduction in CO_2 capture is mostly due to the consideration of uncertainty in the present scenario.

Table 12 Multi-objective multi-period optimization under uncertainty design specifications

	Lower Bound	Upper Bound	1NM point
Height (m)	5.84	6.41	6.0997
Diameter (m)	0.39	0.46	0.44
Capital Cost ($/year)	957	1,233	1,117
Operating Cost ($/year)	5,481	5,481	5,479
Θ_{min} [Annual Cost ($/year)]	6,438	6,714	6,596
Θ_{max} [% CO_2 capture]	85 %	93.70 %	91.16 %

Table 12 also shows that the absorber dimensions (i.e., diameter and height) at the lower bound are 1.4% larger for the optimization under uncertainty than that reported for scenario B's lower bound. On the other hand, the difference in dimensions for the upper bound problem solved in the present scenario is 2.5% larger than those obtained for Scenario B. This nonlinear effect was also observed for the case of robust optimal design under uncertainty; that is, larger equipment sizes are needed at higher (stricter) CO_2 capture rates under process uncertainty.

Figure 14 shows the effects of simulating scenario B's design specifications in the presence of uncertainty. As shown in this figure, the average CO_2 capture under Scenario B's design is 90.87%, which is only 0.3% lower than that obtained from the 1NM solution point for the present scenario. Although this difference in CO_2 capture between Scenario B and Scenario C is relatively small, an additional 3.4 tonnes of annual CO_2 are captured using Scenario C's design when the realizations in the uncertain parameters are set to the worst-case scenario (lowest possible CO_2

capture rate). Similarly, an o from Scenario C's design when the uncertain parameters are set to the more optimistic scenario (i.e. the combination in the uncertain parameters that produces the highest CO_2 capture rate). These results indicate the significance of taking uncertainty and multi-period changes into account while selecting the optimal design specifications and operating policies for a post-combustion CO_2 capture absorber column.

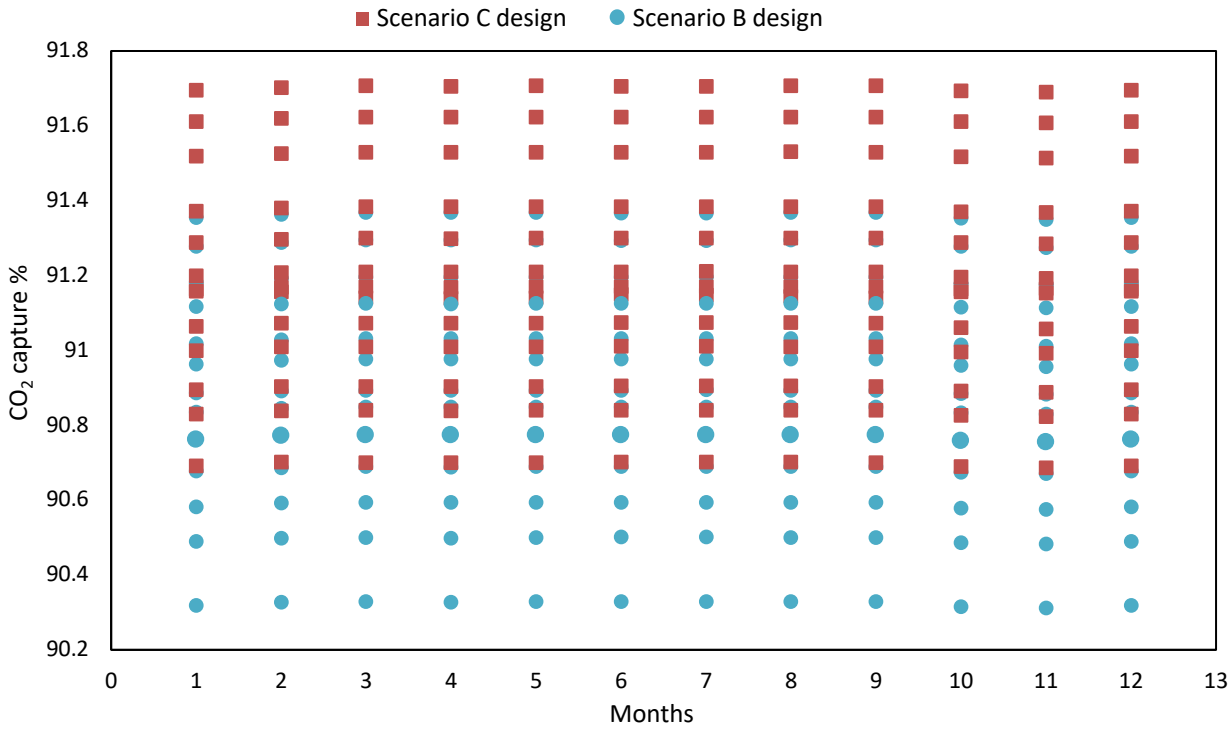

Figure 14 Effect of process uncertainty on the design obtained for Scenario B and C

Considering the actual carbon pricing of 40 \$/tonCO_2 (The World Bank, 2019), the annual costs of CO_2 emissions in the flue gas stream estimated from the present model are approximately 38,000 \$/year. If a post-combustion CO_2 capture process with a minimum CO_2 capture rate of 90% were installed, then the annualized capital and operating costs of the absorber unit for the present scenario would only represent 27% of the original carbon costs, i.e. without a CO_2 capture

process. Note that the annualized costs of the additional post-combustion CO_2 capture units (e.g. stripper and reboiler) and the corresponding plant energy requirements have not been considered and will be the subject of future work.

4.3 Chapter Summary

In this chapter the optimal design and operations management conditions of the CO_2 capture absorber column were studied under a multi-period scenario where seasonal changes in the flowrate of the flue gas entering the CO_2 capture absorber column were considered. The optimization was also evaluated under uncertainty in the composition of the flue gas, in the equilibrium pressure parameter and in the heat of reaction. A bi-objective approach was considered where the aim was to maximize the CO_2 capture and to minimize the column annual costs. An optimal solution under this bi-objective problem was evaluated under different scenarios. The results show that, in order to accommodate process uncertainty and seasonal changes in the power plant's operating conditions, larger annualized costs and lower CO_2 capture rates than those obtained under nominal conditions are expected.

The quantitative differences between the optimal solutions of the scenarios considered in this work may not be relevant; however, those small changes in the design and operating policies are critical to guarantee a feasible operation of this process under uncertainty and seasonal variations in the flue gas stream.

Chapter 5

Conclusions and Recommendations

5.1 Conclusions

The aim of this thesis was to develop studies that consider the optimal design and operations management of a post-combustion CO_2 capture absorber column under process uncertainty. In particular, two studies involving the robust design of the absorber model under static and seasonal changes in the flue gas flowrate were considered in this research. In addition, a multi-objective formulation was formulated with the aim to evaluate the optimal design and operations management under two of the most important objectives for this process, i.e. maximize the CO_2 capture rate and minimize the annualized capital and operating costs of the absorber column. Model parameter uncertainty as well as uncertainty in the input variables were considered in this work. The number of uncertain realizations considered in the optimization formulation is key to most surely ensure a robust optimal process design. Moreover, a more extensive evaluation of the uncertainty effects will also lead to higher computational costs.

Results from this study suggest that larger dimensions in design are required when the optimization was evaluated under uncertainty, which is expected since the design requires to accommodate all the possible uncertainty realizations considered in the formulation. The model was also optimized under nominal conditions, i.e., no uncertainty in the process. The optimization studies showed that the optimal design under nominal conditions was smaller for both single-objective and multi-objective approaches than those obtained from the optimal design under uncertainty. Nevertheless, when the optimal design under nominal conditions was evaluated for potential realizations of the uncertain scenarios; the results showed that those designs may not

comply with the CO_2 emissions targets considered in the optimization formulation. Those results showed that those designs and operation policies may not be suitable for a real-life operation since the design may not satisfy the process design goals, e.g. cannot meet environmental constraints imposed on the plant. Additionally, larger designs were observed in the presence of a large process uncertainty and the design was even larger when more strict CO_2 capture policies were considered. Moreover, when the formulation under uncertainty was optimized for a multi-period scenario under two objectives, the equipment dimensions and annualized costs were larger than the cases where a single period was optimized.

The results from the latter study showed that quantification between optimal dimensions under nominal conditions and under uncertainty may seem not be significant; however, the optimal design considering uncertainty and seasonal changes will be able to comply with the CO_2 capture policies. Larger dimensions may lead to higher annualized costs; however, this design will most surely guarantee that the environmental constraints will be met, thus improving the long term process economics and performance for this process.

5.2 Recommendations

The research presented in this work can be extended to further advance the development and implementation of CO_2 capture technologies. The recommendations considered for this research are as follows:

- In the present work, design optimization under uncertainty was performed using steady-state models. However, in order to simulate the process performance under a period of time, a multi-period approach was established. Furthermore, accounting for the dynamic behaviour of the process will provide new insight into the optimal operation of this

process under uncertainty though high computational demands may be expected. Accordingly, new solution strategies may need to be implemented to alleviate the computational costs associated with the solution of those dynamic optimization problems.

- A single unit of the process was optimized in this study, i.e. the absorber column. This unit plays a crucial role in the process. However, considering other units in the process in order to establish optimal design and operating conditions for the complete process flowsheet is essential for process improvement. Furthermore, considering the optimal solution of the complete CO_2 capture process under uncertainty while using a mechanistic process model will need a specific strategy given the significantly large number of equations that would need to be solved simultaneously. Studies accounting for uncertainty in the complete process will also provide new insight into the optimal operation of this process.
- The multi-scenario method considered for robust optimization in this study will likely guarantee that the optimal design may always be feasible for the possible uncertain scenarios selected. While this is acceptable, the addition of more uncertain parameters in the analysis may lead to the specification of overly conservative solutions. Alternative optimization strategies considering probabilistic distributions in the uncertain parameters such as stochastic programming or chance constraint optimization may be explored to produce attractive solutions that can comply with the process constraints at specific (user-defined) probability limits.

Bibliography

Acevedo, J., Pistikopoulos, E.N., 1998. Stochastic optimization based algorithms for process synthesis under uncertainty. Comput. Chem. Eng. 22, 647–671. https://doi.org/https://doi.org/10.1016/S0098-1354(97)00234-2

AESO, 2017. Annual Market Statistics.

Arellano-Garcia, H., Wozny, G., 2009. Chance constrained optimization of process systems under uncertainty: I. Strict monotonicity. Comput. Chem. Eng. 33, 1568–1583. https://doi.org/https://doi.org/10.1016/j.compchemeng.2009.01.022

Austgen, D.M., Rochelle, G.T., Peng, X., Chen, C.C., 1989. Model of Vapor—Liquid Equilibria for Aqueous Acid Gas—Alkanolamine Systems Using the Electrolyte—NRTL Equation. Ind. Eng. Chem. Res. 28, 1060–1073. https://doi.org/10.1021/ie00091a028

Bahakim, S.S., Rasoulian, S., Ricardez-Sandoval, L.A., 2014. Optimal design of large-scale chemical processes under uncertainty: A ranking-based approach. AIChE J. 60, 3243–3257. https://doi.org/10.1002/aic.14515

Bahakim, S.S., Ricardez-Sandoval, L.A., 2015. Optimal Design of a Postcombustion CO 2 Capture Pilot-Scale Plant under Process Uncertainty : A Ranking-Based Approach. Ind. Eng. Chem. Res. 54, 3879–3892. https://doi.org/10.1021/ie5048253

Bahakim, S.S., Ricardez-Sandoval, L.A., 2014. Simultaneous design and MPC-based control for dynamic systems under uncertainty: A stochastic approach. Comput. Chem. Eng. 63, 66–81. https://doi.org/https://doi.org/10.1016/j.compchemeng.2014.01.002

Bernier, E., Maréchal, F., Samson, R., 2010. Multi-objective design optimization of a natural gas-combined cycle with carbon dioxide capture in a life cycle perspective. Energy. https://doi.org/10.1016/j.energy.2009.06.037

Biegler, L.T., Grossmann, I.E., Westerberg Pittsburgh, PA (United States)], A.W. [Carnegie M.U., 1997. Systematic methods for chemical process design. Prentice Hall, Old Tappan, NJ (United States), United States.

Birge, J.R., Louveaux, F., 1997. Introduction to Stochastic optimization, Introduction to Stochastic Programming. https://doi.org/10.1007/978-1-4614-0237-4

Bui, M., Gunawan, I., Verheyen, V., Feron, P., Meuleman, E., Adeloju, S., 2014. Dynamic modelling and optimisation of flexible operation in post-combustion CO2capture plants-A review. Comput. Chem. Eng. 61, 245–265. https://doi.org/10.1016/j.compchemeng.2013.11.015

C. J. Geankoplis, 1993. Transport Processes and Unit Operations, Prentice-Hall International.

https://doi.org/10.1016/j.bpobgyn.2009.01.007

Chaffart, D., Rasoulian, S., Ricardez-Sandoval, L.A., 2016. Distributional uncertainty analysis and robust optimization in spatially heterogeneous multiscale process systems. AIChE J. 62, 2374–2390. https://doi.org/10.1002/aic.15215

Chu, F., Yang, L., Du, X., Yang, Y., 2016. CO2capture using MEA (monoethanolamine) aqueous solution in coal-fired power plants: Modeling and optimization of the absorbing columns. Energy 109, 495–505. https://doi.org/10.1016/j.energy.2016.04.123

Cignitti, S., Mansouri, S.S., Woodley, J.M., Abildskov, J., 2018. Systematic Optimization-Based Integrated Chemical Product-Process Design Framework. Ind. Eng. Chem. Res. 57, 677–688. https://doi.org/10.1021/acs.iecr.7b04216

Collette, Y., Siarry, P., 2003. Multiobjective optimization : principles and case studies, Decision Engineering. https://doi.org/10.1007/978-3-662-08883-8

Cristóbal, J., Guillén-Gosálbez, G., Jiménez, L., Irabien, A., 2012. Multi-objective optimization of coal-fired electricity production with CO2 capture. Appl. Energy 98, 266–272. https://doi.org/10.1016/j.apenergy.2012.03.036

Engineering, C., Cost, P., 2015. Economic Indicators. Chem. Eng. 122, 80.

Eslick, J.C., Miller, D.C., 2011. A multi-objective analysis for the retrofit of a pulverized coal power plant with a CO2capture and compression process. Comput. Chem. Eng. https://doi.org/10.1016/j.compchemeng.2011.03.020

Fazlollahi, S., Maréchal, F., 2013. Multi-objective, multi-period optimization of biomass conversion technologies using evolutionary algorithms and mixed integer linear programming (MILP). Appl. Therm. Eng. 50, 1504–1513. https://doi.org/10.1016/j.applthermaleng.2011.11.035

GarciÌa-Herreros, P., GoÌmez, J.M., Gil, I.D., RodriÌguez, G., 2011. Optimization of the design and operation of an extractive distillation system for the production of fuel grade ethanol using glycerol as entrainer. Ind. Eng. Chem. Res. 50, 3977–3985. https://doi.org/10.1021/ie101845j

Gáspár, J., Cormoş, A.M., 2011. Dynamic modeling and validation of absorber and desorber columns for post-combustion CO2capture. Comput. Chem. Eng. 35, 2044–2052. https://doi.org/10.1016/j.compchemeng.2010.10.001

Gaspar, J., Loldrup, P., 2016. Simulation and multivariable optimization of post-combustion capture using piperazine. Int. J. Greenh. Gas Control 51, 276–289. https://doi.org/10.1016/j.ijggc.2016.06.003

Giannakoudis, G., Papadopoulos, A.I., Seferlis, P., Voutetakis, S., 2010. Optimum design and

operation under uncertainty of power systems using renewable energy sources and hydrogen storage. Int. J. Hydrogen Energy 35, 872–891. https://doi.org/10.1016/j.ijhydene.2009.11.044

Gomes, U., Patil, B., Betancourt-Torcat, A., Ricardez-Sandoval, L., 2014. Optimal infrastructure of the upgrading operations in the oil sands under uncertainty: A multiscenario MINLP approach. Ind. Eng. Chem. Res. 53, 16406–16424. https://doi.org/10.1021/ie501772j

Grossmann, I.E., Drabbant, R., Jain, R.K., 1982. Incorporating toxicology in the synthesis of industrial chemical complexes. Chem. Eng. Commun. 17, 151–170. https://doi.org/10.1080/00986448208911622

Haghpanah, R., Majumder, A., Nilam, R., Rajendran, A., Farooq, S., Karimi, I.A., Amanullah, M., 2013. Multiobjective optimization of a four-step adsorption process for postcombustion CO2capture via finite volume simulation. Ind. Eng. Chem. Res. 52, 4249–4265. https://doi.org/10.1021/ie302658y

Haimour, N., Sandall, O.C., 1984. Absorption of carbon dioxide into aqueous methyldiethanolamine. Chem. Eng. Sci. 39, 1791–1796. https://doi.org/10.1016/0009-2509(84)80115-3

Harkin, T., Hoadley, A., Hooper, B., 2012. Using multi-objective optimisation in the design of CO2capture systems for retrofit to coal power stations. Energy 41, 228–235. https://doi.org/10.1016/j.energy.2011.06.031

Harun, N., Douglas, P.L., Ricardez-Sandoval, L., Croiset, E., 2011. Dynamic Simulation of MEA Absorption Processes for CO2 Capture from Fossil Fuel Power Plant. Energy Procedia 4, 1478–1485. https://doi.org/10.1016/j.egypro.2011.02.014

Harun, N., Nittaya, T., Douglas, P.L., Croiset, E., Ricardez-Sandoval, L.A., 2012. Dynamic simulation of MEA absorption process for CO2capture from power plants. Int. J. Greenh. Gas Control 10, 295–309. https://doi.org/10.1016/j.ijggc.2012.06.017

He, X., Wang, Y., Bhattacharyya, D., Lima, F. V., Turton, R., 2017. Dynamic Modeling and Advanced Control of Post-Combustion CO 2 Capture Plants. Chem. Eng. Res. Des. 1, 430–439. https://doi.org/10.1016/j.cherd.2017.12.020

Hikita, H., Asai, S., Ishikawa, H., Honda, M., 1977. The kinetics of reactions of carbon dioxide with monoethanolamine, diethanolamine and triethanolamine by a rapid mixing method. Chem. Eng. J. 13, 7–12. https://doi.org/10.1016/0300-9467(77)80002-6

Hoff, K.A., Juliussen, O., Falk-Pedersen, O., Svendsen, H.F., 2004. Modeling and experimental study of carbon dioxide absorption in aqueous alkanolamine solutions using a membrane contactor. Ind. Eng. Chem. Res. 43.

Huertas, J.I., Gomez, M.D., Giraldo, N., Garzón, J., 2015. CO2 Absorbing Capacity of MEA. J. Chem.

2015. https://doi.org/https://doi.org/10.1155/2015/965015.

Kang, C.A., Brandt, A.R., Durlofsky, L.J., Jayaweera, I., 2016. Assessment of advanced solvent-based post-combustion CO2 capture processes using a bi-objective optimization technique. Appl. Energy 179, 1209–1219.

Karuppiah, R., Grossmann, I.E., 2006. Global optimization of multiscenario mixed integer nonlinear programming models arising in the synthesis of integrated water networks under uncertainty. Comput. Aided Chem. Eng. 21, 1747–1752. https://doi.org/10.1016/S1570-7946(06)80300-7

Koller, R.W., Ricardez-Sandoval, L.A., Biegler, L.T., 2018. Stochastic back-off algorithm for simultaneous design, control, and scheduling of multiproduct systems under uncertainty. AIChE J. 64, 2379–2389. https://doi.org/10.1002/aic.16092

Kvamsdal, H.M., Jakobsen, J.P., Hoff, K.A., 2009. Dynamic modeling and simulation of a CO2 absorber column for post-combustion CO2 capture. Chem. Eng. Process. Process Intensif. 48, 135–144. https://doi.org/10.1016/j.cep.2008.03.002

Kvamsdal, H.M., Rochelle, G.T., 2008. Effects of the temperature bulge in CO2 absorption from flue gas by aqueous monoethanolamine. Ind. Eng. Chem. Res. 47, 867–875. https://doi.org/10.1021/ie061651s

Laird, C.D., Biegler, L.T., 2008. Large-Scale Nonlinear Programming for Multi-scenario Optimization. Model. Simul. Optim. complex Process. 323–336. https://doi.org/10.1007/978-3-540-79409-7_22

Lawal, A., Wang, M., Stephenson, P., Yeung, H., 2009. Dynamic modelling of CO2 absorption for post combustion capture in coal-fired power plants. Fuel 88, 2455–2462. https://doi.org/10.1016/j.fuel.2008.11.009

Lee, A.S., Eslick, J.C., Miller, D.C., Kitchin, J.R., 2013. Comparisons of amine solvents for post-combustion CO2 capture: A multi-objective analysis approach. Int. J. Greenh. Gas Control 18, 68–74. https://doi.org/10.1016/j.ijggc.2013.06.020

Li, H., Maréchal, F., Burer, M., Favrat, D., 2006. Multi-objective optimization of an advanced combined cycle power plant including CO2separation options. Energy 31, 3117–3134. https://doi.org/10.1016/j.energy.2006.03.014

Li, P., Arellano-Garcia, H., Wozny, G., 2008. Chance constrained programming approach to process optimization under uncertainty. Comput. Chem. Eng. 32, 25–45. https://doi.org/https://doi.org/10.1016/j.compchemeng.2007.05.009

Li Yuen Fong, J.C., Anderson, C.J., Xiao, G., Webley, P.A., Hoadley, A.F.A., 2016. Multi-objective optimisation of a hybrid vacuum swing adsorption and low-temperature post-combustion CO2capture. J. Clean. Prod. https://doi.org/10.1016/j.jclepro.2015.08.033

Li, Z., Floudas, C.A., 2016. Optimal scenario reduction framework based on distance of uncertainty distribution and output performance: II. Sequential reduction. Comput. Chem. Eng. 84, 599–610. https://doi.org/10.1016/j.compchemeng.2015.05.010

Li, Z., Ierapetritou, M.G., 2008. Robust Optimization for Process Scheduling Under Uncertainty. Ind. Eng. Chem. Res. 47, 4148–4157. https://doi.org/10.1021/ie071431u

Liang, Z. (Henry), Rongwong, W., Liu, H., Fu, K., Gao, H., Cao, F., Zhang, R., Sema, T., Henni, A., Sumon, K., Nath, D., Gelowitz, D., Srisang, W., Saiwan, C., Benamor, A., Al-Marri, M., Shi, H., Supap, T., Chan, C., Zhou, Q., Abu-Zahra, M., Wilson, M., Olson, W., Idem, R., Tontiwachwuthikul, P. (PT), 2015. Recent progress and new developments in post-combustion carbon-capture technology with amine based solvents. Int. J. Greenh. Gas Control. https://doi.org/10.1016/j.ijggc.2015.06.017

Lin, X., Janak, S.L., Floudas, C.A., 2004. A new robust optimization approach for scheduling under uncertainty : I . Bounded uncertainty 28, 1069–1085. https://doi.org/10.1016/j.compchemeng.2003.09.020

Mac Dowell, N., Shah, N., 2015. The multi-period optimisation of an amine-based CO2capture process integrated with a super-critical coal-fired power station for flexible operation. Comput. Chem. Eng. 74, 169–183. https://doi.org/10.1016/j.compchemeng.2015.01.006

Mac Dowell, N., Shah, N., 2013. Identification of the cost-optimal degree of CO2capture: An optimisation study using dynamic process models. Int. J. Greenh. Gas Control 13, 44–58. https://doi.org/10.1016/j.ijggc.2012.11.029

Mansouri, S.S., Sales-Cruz, M., Huusom, J.K., Gani, R., 2016. Systematic integrated process design and control of reactive distillation processes involving multi-elements. Chem. Eng. Res. Des. 115, 348–364. https://doi.org/10.1016/j.cherd.2016.07.010

Marler, R.T., Arora, J.S., 2007. Survey of multi-objective optimization methods for engineering. Struct. Multidiscip. Optim. 52, 91–95. https://doi.org/10.1007/s00158-003-0368-6

McCulloch, S., Keeling, S., Malischek, R., Stanley, T., 2016. 20 Years of Carbon Capture and Storage - Accelerating Future Deployment, International Energy Agency. https://doi.org/10.1787/9789264267800-en

Mores, P., Scenna, N., Mussati, S., 2012. CO2capture using monoethanolamine (MEA) aqueous solution: Modeling and optimization of the solvent regeneration and CO2desorption process. Energy 45, 1042–1058. https://doi.org/10.1016/j.energy.2012.06.038

Mores, P.L., Manassaldi, J.I., Scenna, N.J., Caballero, J.A., Mussati, M.C., Mussati, S.F., 2018. Optimization of the design, operating conditions, and coupling configuration of combined cycle power plants and CO 2 capture processes by minimizing the mitigation cost. Chem. Eng. J. 331, 870–894. https://doi.org/10.1016/j.cej.2017.08.111

N. Mac Dowell, N.J. Samsatli, N.S., 2013. Dynamic modelling and analysis of an amine-based post-combustion CO2 capture absorption column. Carbohydr. Res. 344, 1032–1033. https://doi.org/10.1016/j.ijggc.2012.10.013

National Energy Board, 2017. Canada's Renewable Power Landscape 2017 – Energy Market Analysis, Energy Economics. https://doi.org/10.1016/0140-9883(82)90045-7

Nittaya, T., Douglas, P.L., Croiset, E., Ricardez-sandoval, L.A., 2014. Dynamic modelling and control of MEA absorption processes for CO 2 capture from power plants. Fuel 116, 672–691. https://doi.org/http://dx.doi.org/10.1016/j.fuel.2013.08.031

Nwaoha, C., Supap, T., Idem, R., Saiwan, C., Tontiwachwuthikul, P., AL-Marri, M.J., Benamor, A., 2017. Advancement and new perspectives of using formulated reactive amine blends for post-combustion carbon dioxide (CO2) capture technologies. https://doi.org/10.1016/j.petlm.2016.11.002

Onda, K., Takeuchi, H., Okumoto, Y., 1968. Mass transfer coefficients between gas and liquid phases in packed columns. J. Chem. Eng. Japan 1, 56–62. https://doi.org/10.1252/jcej.1.56

Ostrovsky, G.M., Ziyatdinov, N.N., Lapteva, T. V, 2013. Optimal design of chemical processes with chance constraints. Comput. Chem. Eng. 59, 74–88. https://doi.org/10.1016/j.compchemeng.2013.05.029

Ostrovsky, G.M., Ziyatdinov, N.N., Lapteva, T. V, Zaitsev, I., 2011. Two-stage optimization problem with chance constraints. Chem. Eng. Sci. 66, 3815–3828. https://doi.org/https://doi.org/10.1016/j.ces.2011.05.001

Patil, B.P., Maia, E., Ricardez-Sandoval, L.A., 2015. Integration of scheduling, design, and control of multiproduct chemical processes under uncertainty. AIChE J. 61, 2456–2470. https://doi.org/10.1002/aic.14833

Pintarič, Z.N., Kravanja, Z., 2004. A strategy for MINLP synthesis of flexible and operable processes 28, 1105–1119. https://doi.org/10.1016/j.compchemeng.2003.09.010

Prölß, K., Tummescheit, H., Velut, S., Åkesson, J., Ab, M., Park, I.S., 2011. Dynamic model of a post-combustion absorption unit for use in a non-linear model predictive control scheme 00. https://doi.org/10.1016/j.egypro.2011.02.161

Quadrelli, R., Peterson, S., 2007. The energy–climate challenge: Recent trends in CO2 emissions from fuel combustion. Energy Policy 35, 5938–5952. https://doi.org/10.1016/j.enpol.2007.07.001

Rafiei, M., Ricardez-Sandoval, L.A., 2018. Stochastic Back-Off Approach for Integration of Design and Control under Uncertainty. Ind. Eng. Chem. Res. 57, 4351–4365. https://doi.org/10.1021/acs.iecr.7b03935

Rangaiah, G.P., 2009. Multi-Objective Optimization in Chemical Engineering-Developments and Applications. Igarss World Scientific Publishing Co. Pte. Ltd. https://doi.org/10.1007/s13398-014-0173-7.2

Reid, R.C., Prausnitz, J.M., Sherwood, T.K., 1977. The properties of gases and liquids. McGraw-Hill (1977). https://doi.org/10.1002/aic.690240634

Ricardez-Sandoval, L.A., 2012. Optimal design and control of dynamic systems under uncertainty: A probabilistic approach. Comput. Chem. Eng. 43, 91–107. https://doi.org/https://doi.org/10.1016/j.compchemeng.2012.03.015

Ricardez-Sandoval, L.A., Budman, H.M., Douglas, P.L., 2009. Integration of design and control for chemical processes: A review of the literature and some recent results. Annu. Rev. Control 33, 158–171. https://doi.org/10.1016/j.arcontrol.2009.06.001

Rochelle, G.T., 2009. Amine Scrubbing for CO2 Capture. Science (80-.). https://doi.org/10.1126/science.1176731

Sahinidis, N. V., 2004. Optimization under uncertainty: State-of-the-art and opportunities. Comput. Chem. Eng. 28, 971–983. https://doi.org/10.1016/j.compchemeng.2003.09.017

Singh, D., Croiset, E., Douglas, P.L., Douglas, M.A., 2003. Techno-economic study of CO2 capture from an existing coal-fired power plant: MEA scrubbing vs. O2/CO2 recycle combustion. Energy Convers. Manag. 44, 3073–3091. https://doi.org/10.1016/S0196-8904(03)00040-2

Smith, J.M., Van Ness, H.C., Abbott, M.M., 2005. Introduction to chemical engineering thermodynamics. McGraw-Hill, Boston.

Tan, L.S., Shariff, a. M., Lau, K.K., Bustam, M. a., 2012. Factors affecting CO2 absorption efficiency in packed column: A review. J. Ind. Eng. Chem. 18, 1874–1883. https://doi.org/10.1016/j.jiec.2012.05.013

te Riele, M.J.M., Snijder, E.D., van Swaaij, W.P.M., 1995. Diffusion Coefficients of CO, CO2, N2O, and N2in Ethanol and Toluene. J. Chem. Eng. Data 40, 37–39. https://doi.org/10.1021/je00017a010

The World Bank, 2019. Carbon Pricing [WWW Document]. World Bank.

Thouchprasitchai, N., Pintuyothin, N., Pongstabodee, S., 2018. Optimization of CO2adsorption capacity and cyclical adsorption/desorption on tetraethylenepentamine-supported surface-modified hydrotalcite. J. Environ. Sci. (China) 65, 293–305. https://doi.org/10.1016/j.jes.2017.02.015

Wang, M., Lawal, A., Stephenson, P., Sidders, J., Ramshaw, C., 2011. Post-combustion CO2 capture with chemical absorption: A state-of-the-art review. Chem. Eng. Res. Des. 89,

1609–1624. https://doi.org/10.1016/j.cherd.2010.11.005

Wiecek, M.M., Blouin, V.Y., Fadel, G.M., Engau, A., Hunt, B.J., Singh, V., 2009. Multi-scenario multi-objective optimization with applications in engineering design. Lect. Notes Econ. Math. Syst. 618, 283–298. https://doi.org/10.1007/978-3-540-85646-7_26

Yuan, Y., Li, Z., Huang, B., 2016. Robust optimization under correlated uncertainty: Formulations and computational study. Comput. Chem. Eng. 85, 58–71. https://doi.org/10.1016/j.compchemeng.2015.10.017

Zhu, Y., Legg, S., Laird, C.D., 2010. Optimal design of cryogenic air separation columns under uncertainty. Comput. Chem. Eng. 34, 1377–1384. https://doi.org/10.1016/j.compchemeng.2010.02.007